MIT Open Access Articles

Preheating after multifield inflation with nonminimal couplings. I. Covariant formalism and attractor behavior

Massachusetts Institute of Technology

Preheating after multifield inflation with nonminimal couplings. I. Covariant formalism and attractor behavior

Matthew P. DeCross,[1,*] David I. Kaiser,[1,†] Anirudh Prabhu,[1,‡] Chanda Prescod-Weinstein,[2,§] and Evangelos I. Sfakianakis[3,‖]

[1]*Department of Physics, Massachusetts Institute of Technology, Cambridge, Massachusetts 02139, USA*
[2]*Department of Physics, University of Washington, Seattle, Washington 98195-1560, USA*
[3]*Department of Physics, University of Illinois at Urbana-Champaign, Urbana, Illinois 61801, USA*

This is the first of a three-part series of papers, in which we study the preheating phase for multifield models of inflation involving nonminimal couplings. In this paper, we study the single-field attractor behavior that these models exhibit during inflation and quantify its strength and parameter dependence. We further demonstrate that the strong single-field attractor behavior persists after the end of inflation. Preheating in such models therefore generically avoids the "dephasing" that typically affects multifield models with minimally coupled fields, allowing efficient transfer of energy from the oscillating inflaton condensate(s) to coupled perturbations across large portions of parameter space. We develop a doubly covariant formalism for studying the preheating phase in such models and identify several features specific to multifield models with nonminimal couplings, including effects that arise from the nontrivial field-space manifold. In papers II and III, we apply this formalism to study how the amplification of adiabatic and isocurvature perturbations varies with parameters, highlighting several distinct regimes depending on the magnitude of the nonminimal couplings ξ_I.

I. INTRODUCTION

This is the first paper in a three-part series that examines the early stages of postinflation reheating in models that involve multiple scalar fields, each nonminimally coupled to gravity. (The companion papers are Refs. [1,2].)

Postinflation reheating is a critical phase in the history of the cosmos, necessary to connect early-Universe inflation to the usual successes of the standard hot big bang scenario. Reheating falls between two regimes that are well constrained by observations, and which match the latest observations remarkably well: production of a spatially flat universe seeded with nearly scale-invariant primordial curvature perturbations during inflation [3–10], and production of specific abundances of light nuclei during big-bang nucleosynthesis [11–13]. Though it remains difficult to relate the reheating phase directly to specific, testable predictions for observations, the process of reheating remains critical in order to compare predictions from the inflationary era with present-day observations, since relating comoving scales at different cosmological epochs requires knowledge of the intervening expansion history of the Universe [14–21]. See [4,22–25] for recent reviews of reheating.

The postinflation reheating phase not only must bring the early Universe to thermal equilibrium in a radiation-dominated phase at an appropriately high temperature, but reheating should also populate the Universe with matter like the kind we see around us today. During inflation, the energy density of the Universe was presumably dominated by one or more scalar "inflaton" fields. After reheating, the energy density should include contributions from multiple species of matter, including the Standard Model particles or (at least) types of matter that decay into Standard Model particles prior to big-bang nucleosynthesis. Such interactions could address other longstanding challenges in cosmological theory, such as generating the observed baryon-antibaryon asymmetry [26–29]. Reheating therefore must be a multifield phenomenon.

Arguably, inflation itself should be treated as a process involving multiple fields. Realistic models of high-energy particle physics typically include many distinct scalar fields at high energies [30–34]. Hence we consider multiple scalar fields to be a central ingredient of realistic models of inflation. Nonminimal couplings between the scalar fields and the Ricci spacetime curvature scalar are also a generic feature of realistic models of the early Universe. Many theoretical motivations for nonminimal couplings derive

---

[*]mdecross@sas.upenn.edu
Now at the Department of Physics and Astronomy, University of Pennsylvania.
[†]dikaiser@mit.edu
[‡]aniprabhu@stanford.edu
Now at the Department of Physics, Stanford University.
[§]cprescod@uw.edu
[‖]evans@nikhef.nl
Now at NIKHEF and Leiden University.

023526-1

from high-energy model building, including dilatons and moduli fields, but a more basic motivation comes from renormalization: as has long been known, models with self-interacting scalar fields in curved spacetime require non-minimal couplings as counterterms in order to remain self-consistent at high energies. Nonminimal couplings are induced by quantum corrections even in the absence of bare couplings; they are a generic feature of scalar fields in curved spacetime [35–41]. Moreover, such couplings arise even in a classical background spacetime. Thus their effects can be important at energy scales relevant to inflationary or postinflationary dynamics, even for models in which quantum-gravitational corrections to the Einstein-Hilbert action—which would presumably be quadratic or higher order in the spacetime curvature—may remain subdominant at those energy scales [42].

In recent work [44–47] we have studied the dynamics during inflation from multifield models with nonminimal couplings, including generalizations of "Higgs inflation" [48]. These papers have demonstrated that such models generically predict observable quantities (related to the spectrum of primordial curvature perturbations) squarely in the most-favored region of the latest observations. Moreover, such models exhibit a strong attractor behavior: across broad regions of parameter space and phase space the fields relax to an effectively single-field trajectory early in inflation. Hence the predictions for observable quantities from these models show little dependence on coupling constants or initial conditions [46]. Such attractor behavior is a generic feature of multifield models with nonminimal couplings, including the so-called "α attractors" [49].

In this paper we focus on the dynamics of such models immediately after inflation, during the "preheating" phase. During preheating, the scalar-field condensate(s) that drove inflation decay resonantly into higher-momentum quanta. We develop a doubly covariant formalism that incorporates metric perturbations and field fluctuations self-consistently (to first order), and which also respects the reparametrization freedom of the nontrivial field-space manifold. We restrict our attention to the early stages of preheating, for which an approximation linear in the fields' fluctuations remains reliable, and only consider decays into scalar fields rather than fermions or gauge fields. Our approach complements previous studies that have examined reheating in models with nonminimally coupled fields [50–56], including Higgs inflation [57–60], as well as with noncanonical kinetic terms or other string-inspired features of the action [61–65]. In our companion papers [1,2], we analyze the amplification of perturbations in this family of models semianalytically and numerically across wide regions of parameter space.

We find three principal distinctions from the well-studied cases of preheating with minimally coupled fields. First, the conformal stretching of the scalar fields' potential in the Einstein frame affects the oscillations of the background fields, compared to the case of minimal couplings. In particular, for strong nonminimal couplings $\xi_I \gg 1$, the background fields' oscillations interpolate between the behavior of minimally coupled models with quadratic and quartic self-couplings. Second, the single-field attractor behavior during inflation typically leads to greater efficiency during preheating than in corresponding multifield models with minimal couplings, in which dephasing of the background fields' oscillations usually damps resonances [24,66,67]. Third, the nontrivial field-space manifold contributes differently to the effective masses for fluctuations in the adiabatic and isocurvature directions, leading to distinct behavior depending on whether the nonminimal couplings are small [$\xi_I < \mathcal{O}(1)$], intermediate [$\xi_I \sim \mathcal{O}(1\text{–}10)$], or large [$\xi_I \geq \mathcal{O}(100)$].

In Sec. II we review the doubly covariant formalism with which we study the dynamics of background fields and fluctuations. In Sec. III we examine the background dynamics for a two-field model during and after inflation, highlighting distinctions between oscillations during preheating with and without nonminimal couplings. The behavior of the background fields during the oscillating phase is critical for understanding the resonant production of particles during preheating. In Sec. IV we introduce a covariant mode expansion for the fluctuations and derive multifield generalizations of the "adiabatic parameter" with which to characterize the resonant, nonperturbative growth of fluctuations. Concluding remarks follow in Sec. V.

II. DOUBLY COVARIANT FORMALISM

When studying multifield models with nonminimal couplings, one must consider two types of gauge transformations: the usual spacetime coordinate transformations, $x^\mu \to x^{\mu\prime}$, as well as transformations of the field-space coordinates, $\phi^I \to \phi^{I\prime}$. To address the first type of transformation, we adopt the usual (spacetime) gauge-invariant perturbation formalism [68–70]; see Refs. [4,71,72] for reviews. To address the multifield aspects, we build on the methods of Refs. [31,73–83]. Together, these yield a doubly covariant formalism for studying fluctuations in these multifield models [44].

We follow closely the notation and parametrization of [44–47]. We work in $(3 + 1)$ spacetime dimensions and adopt the spacetime metric signature $(-, +, +, +)$. We consider models with N real-valued scalar fields, each of which is coupled to the Ricci spacetime curvature scalar. In the Jordan frame, the action takes the form

$$S = \int d^4x \sqrt{-\tilde{g}} \left[f(\phi^I)\tilde{R} - \frac{1}{2}\delta_{IJ}\tilde{g}^{\mu\nu}\partial_\mu\phi^I\partial_\nu\phi^J - \tilde{V}(\phi^I) \right],$$

(1)

where uppercase Latin letters label field-space indices, $I, J = 1, 2, \ldots, N$, Greek letters label spacetime indices, μ,

$\nu = 0, 1, 2, 3$, and tildes denote Jordan-frame quantities. We will use lowercase Latin letters for spatial indices, $i, j = 1, 2, 3$.

We may perform a conformal transformation to bring the gravitational portion of the action into canonical Einstein-Hilbert form, by rescaling $\tilde{g}_{\mu\nu}(x) \to g_{\mu\nu}(x) = \Omega^2(x)\tilde{g}_{\mu\nu}(x)$. The conformal factor $\Omega^2(x)$ is related to the nonminimal-coupling function,

$$g_{\mu\nu}(x) = \frac{2}{M_{\rm pl}^2} f(\phi^I(x))\tilde{g}_{\mu\nu}(x), \qquad (2)$$

where $M_{\rm pl} \equiv 1/\sqrt{8\pi G} = 2.43 \times 10^{18}$ GeV is the reduced Planck mass. The action may then be rewritten [84]

$$S = \int d^4x \sqrt{-g}\left[\frac{M_{\rm pl}^2}{2}R - \frac{1}{2}\mathcal{G}_{IJ}(\phi^K)g^{\mu\nu}\partial_\mu\phi^I\partial_\nu\phi^J - V(\phi^I)\right]. \qquad (3)$$

(See also Ref. [85].) The potential in the Einstein frame is stretched by the conformal factor,

$$V(\phi^I) = \frac{M_{\rm pl}^4}{4f^2(\phi^I)}\tilde{V}(\phi^I). \qquad (4)$$

In addition, the nonminimal couplings induce a curved field-space manifold in the Einstein frame, with associated field-space metric $\mathcal{G}_{IJ}(\phi^K)$. Because the induced field-space manifold is not conformal to flat for $N \geq 2$, no combination of rescalings of $g_{\mu\nu}$ and ϕ^I can retain the Einstein-Hilbert form for the gravitational portion of the action while also bringing the fields' kinetic terms into canonical form [84]. The components of $\mathcal{G}_{IJ}$ take the form

$$\mathcal{G}_{IJ}(\phi^K) = \frac{M_{\rm pl}^2}{2f(\phi^K)}\left[\delta_{IJ} + \frac{3}{f(\phi^K)}f_{,I}f_{,J}\right], \qquad (5)$$

where $f_{,I} = \partial f/\partial\phi^I$. The field-space metric satisfies $\mathcal{G}^{IJ}\mathcal{G}_{JK} = \delta^I{}_K$, and field-space indices are raised and lowered with $\mathcal{G}_{IJ}$.

Varying the action of Eq. (3) with respect to $g_{\mu\nu}$ yields the field equations

$$R_{\mu\nu} - \frac{1}{2}g_{\mu\nu}R = \frac{1}{M_{\rm pl}^2}T_{\mu\nu}, \qquad (6)$$

with the energy-momentum tensor given by [44]

$$T_{\mu\nu} = \mathcal{G}_{IJ}\partial_\mu\phi^I\partial_\nu\phi^J - g_{\mu\nu}\left[\frac{1}{2}\mathcal{G}_{IJ}g^{\alpha\beta}\partial_\alpha\phi^I\partial_\beta\phi^J + V(\phi^I)\right]. \qquad (7)$$

Varying Eq. (3) with respect to ϕ^I yields the equation of motion

$$\Box\phi^I + g^{\mu\nu}\Gamma^I{}_{JK}\partial_\mu\phi^J\partial_\nu\phi^K - \mathcal{G}^{IJ}V_{,J} = 0, \qquad (8)$$

where $\Box\phi^I \equiv g^{\mu\nu}\phi^I{}_{;\mu\nu}$ and $\Gamma^I{}_{JK}(\phi^L)$ is the Christoffel symbol constructed from the field-space metric $\mathcal{G}_{IJ}$.

We expand the scalar fields and the spacetime metric to first order in perturbations. We are interested in the behavior of the fields at the end of inflation, so we consider scalar metric perturbations around a spatially flat Friedmann-Lemaître-Robertson-Walker (FLRW) line element,

$$\begin{aligned}ds^2 &= g_{\mu\nu}(x)dx^\mu dx^\nu \\ &= -(1+2A)dt^2 + 2a(\partial_i B)dx^i dt \\ &\quad + a^2[(1-2\psi)\delta_{ij} + 2\partial_i\partial_j E]dx^i dx^j,\end{aligned} \qquad (9)$$

where $a(t)$ is the scale factor. We also expand the fields,

$$\phi^I(x^\mu) = \varphi^I(t) + \delta\phi^I(x^\mu). \qquad (10)$$

The fluctuations $\delta\phi^I$ represent finite displacements from the fields' classical trajectory through field space; the fluctuations $\delta\phi^I$ are gauge dependent with respect to both $x^\mu \to x^{\mu\prime}$ and $\varphi^I \to \varphi^{I\prime}$. We therefore proceed in two steps. First, following Ref. [82], we introduce a vector $\mathcal{Q}^I$ to represent the field fluctuations covariantly with respect to the field-space metric, $\mathcal{G}_{IJ}$. (See also Ref. [83].) The field-space vectors $\phi^I(x^\mu)$ and $\varphi^I(t)$ may be connected by a geodesic along the field-space manifold with some affine parameter λ. We take $\phi^I(\lambda = 0) = \varphi^I$ and $\phi^I(\lambda = \epsilon) = \varphi^I + \delta\phi^I$. (We may take $\epsilon = 1$ at the end.) These boundary conditions uniquely specify the vector $\mathcal{Q}^I$ that connects ϕ^I and φ^I, such that $\phi^I|_{\lambda=0} = \varphi^I$ and $\mathcal{D}_\lambda\phi^I|_{\lambda=0} = (d\phi^I/d\lambda)|_{\lambda=0} = \mathcal{Q}^I$, where $\mathcal{D}_\lambda$ is a covariant derivative with respect to the affine parameter. Then [82]

$$\delta\phi^I = \mathcal{Q}^I - \frac{1}{2!}\Gamma^I{}_{JK}\mathcal{Q}^J\mathcal{Q}^K + \frac{1}{3!}[\Gamma^I{}_{LM}\Gamma^M{}_{JK} - \Gamma^I{}_{JK;L}] \\ \times \mathcal{Q}^J\mathcal{Q}^K\mathcal{Q}^L + \cdots \qquad (11)$$

where the $\Gamma^I{}_{JK}$ are evaluated at background order, as functions of φ^I. Note that $\delta\phi^I \to \mathcal{Q}^I$ to first order in fluctuations, but one must take care to distinguish the two when working to higher order, as we will do in Sec. IV A when we expand the action to second order in $\mathcal{Q}^I$. Next, we follow Ref. [44] and define a linear combination of $\mathcal{Q}^I$ and the metric perturbation ψ to form a generalization of the gauge-invariant Mukhanov-Sasaki variable:

$$Q^I \equiv \mathcal{Q}^I + \frac{\dot{\varphi}^I}{H}\psi. \qquad (12)$$

The vector Q^I is doubly covariant, with respect to spacetime gauge transformations (to first order in metric perturbations) as well as transformations of the field-space coordinates φ^I.

To first order in perturbations, $Q^I \to \mathcal{Q}^I \to \delta\phi^I$ in the spatially flat gauge.

For an arbitrary vector in the field space, A^I, we may define the usual covariant derivative with respect to the field-space metric,

$$\mathcal{D}_J A^I = \partial_J A^I + \Gamma^I_{JK} A^K, \qquad (13)$$

and a (covariant) directional derivative with respect to the affine parameter, cosmic time, t,

$$\mathcal{D}_t A^I \equiv \dot{\varphi}^J \mathcal{D}_J A^I = \dot{A}^I + \Gamma^I_{JK} \dot{\varphi}^J A^K, \qquad (14)$$

where overdots denote partial derivatives with respect to t. To background order, we may then write the equation of motion for the fields φ^I from Eq. (8),

$$\mathcal{D}_t \dot{\varphi}^I + 3H\dot{\varphi}^I + \mathcal{G}^{IJ} V_{,J} = 0, \qquad (15)$$

while Eqs. (6) and (7) yield the usual dynamical equations at background order,

$$H^2 = \frac{1}{3M^2_{\text{pl}}} \left[\frac{1}{2} \mathcal{G}_{IJ} \dot{\varphi}^I \dot{\varphi}^J + V(\varphi^I) \right],$$

$$\dot{H} = -\frac{1}{2M^2_{\text{pl}}} \mathcal{G}_{IJ} \dot{\varphi}^I \dot{\varphi}^J. \qquad (16)$$

In Eqs. (15) and (16), $H \equiv \dot{a}/a$ is the Hubble parameter, and the field-space metric is evaluated at background order, $\mathcal{G}_{IJ}(\varphi^K)$.

To first order in Q^I, Eqs. (6)–(8) may be combined to yield the equation of motion for the gauge-invariant perturbations [44,80,86]

$$\mathcal{D}_t^2 Q^I + 3H\mathcal{D}_t Q^I + \left[\frac{k^2}{a^2} \delta^I{}_J + \mathcal{M}^I{}_J \right] Q^J = 0, \quad (17)$$

where the mass-squared tensor takes the form

$$\mathcal{M}^I{}_J \equiv \mathcal{G}^{IK}(\mathcal{D}_J \mathcal{D}_K V) - \mathcal{R}^I{}_{LMJ} \dot{\varphi}^L \dot{\varphi}^M$$
$$- \frac{1}{M^2_{\text{pl}} a^3} \mathcal{D}_t \left(\frac{a^3}{H} \dot{\varphi}^I \dot{\varphi}_J \right) \qquad (18)$$

and $\mathcal{R}^I{}_{LMJ}$ is the Riemann tensor for the field-space manifold. All expressions in Eqs. (17) and (18) involving $\mathcal{G}_{IJ}$, V, and their derivatives are evaluated at background order in the fields, φ^I. The term in Eq. (18) that is proportional to $1/M^2_{\text{pl}}$ arises from the coupled metric perturbations.

III. COUPLINGS AND BACKGROUND DYNAMICS

Renormalization of models with self-coupled scalar fields in curved spacetime requires counter-terms of the

form $\xi\phi^2 R$ for each nonminimally coupled field [35–41]. Here we consider a two-field model, $\phi^I = \{\phi, \chi\}^T$, and take $f(\phi^I)$ to be of the form

$$f(\phi, \chi) = \frac{1}{2}[M^2_{\text{pl}} + \xi_\phi \phi^2 + \xi_\chi \chi^2]. \qquad (19)$$

Each scalar field ϕ^I couples to the Ricci scalar with its own nonminimal-coupling constant, ξ_I; conformal coupling corresponds to $\xi_I = -1/6$. The field-space metric, $\mathcal{G}_{IJ}(\varphi^K)$, is determined by the form of $f(\phi^I)$ and its derivatives, as in Eq. (5). Explicit expressions for $\mathcal{G}_{IJ}$ and related quantities for this model may be found in Appendix A.

We consider a simple, renormalizable form for the potential in the Jordan frame,

$$\tilde{V}(\phi, \chi) = \frac{\lambda_\phi}{4}\phi^4 + \frac{g}{2}\phi^2\chi^2 + \frac{\lambda_\chi}{4}\chi^4. \qquad (20)$$

We take $\lambda_I > 0$ and neglect bare masses m_I^2, in order to focus on effects from the quartic self-couplings and direct interaction terms within a parameter space of manageable size. The effects from nonzero m_I^2 may be incorporated using the methods developed here.

Several types of considerations may be used to bound the range of ξ_I of interest. Perhaps most fundamentally, vacuum stability (under renormalization-group flow) requires $\xi_I \geq -0.03$ [87]. Meanwhile, earlier studies of single-field models had found that $|\xi| \leq 10^{-3}$ for $\xi < 0$ in order to yield sufficient inflation [88–92]. These constraints leave a very narrow window of parameter space for $\xi_I < 0$ that could still be viable. Moreover, as we will see below, the behavior of such models with $|\xi_I| \ll 1$ tends to show only modest departures from the well-studied minimally coupled case, whereas qualitatively new behavior arises for $|\xi_I| \gg 1$. Hence we restrict our attention here to positive couplings, $\xi_I > 0$.

Next we may consider observational constraints, such as the present bound on the primordial tensor-to-scalar ratio, $r \leq 0.1$ [93], which corresponds to the bound $H_* \leq 3.4 \times 10^{-5} M_{\text{pl}}$. (Asterisks indicate values of quantities at the time during inflation when observationally relevant perturbations first crossed outside the Hubble radius.) Models in our class predict [44–47]

$$r = \frac{16\epsilon}{1 + T^2_{\mathcal{RS}}}, \qquad (21)$$

where ϵ is the usual slow-roll parameter,

$$\epsilon \equiv -\frac{\dot{H}}{H^2}, \qquad (22)$$

and $T^2_{\mathcal{RS}}$ is the transfer function for long-wavelength modes between the adiabatic ($\mathcal{R}$) and isocurvature ($\mathcal{S}$) directions.

As analyzed in Refs. [44–47] and discussed further in the next subsection, models in this class generically display strong single-field attractor behavior. Within an attractor the background fields' trajectory does not turn, and hence $T_{\mathcal{RS}}^2 \to 0$. Furthermore, given our covariant framework, we may consider the case in which the fields move along the direction $\chi = 0$ during inflation without loss of generality. In the limit $\xi_\phi \gg 1$, we find to good approximation [46]

$$H_* \simeq \sqrt{\frac{\lambda_\phi}{12\xi_\phi^2}} M_{\rm pl}, \qquad N_* \simeq \frac{3}{4}\delta_*^2, \qquad \epsilon \simeq \frac{3}{4N_*^2}, \quad (23)$$

where

$$\delta^2 \equiv \frac{\xi_\phi \phi^2}{M_{\rm pl}^2}, \qquad (24)$$

and N_* is the number of efolds before the end of inflation when relevant scales crossed outside the Hubble radius. (See also Ref. [94].) Assuming $50 \leq N_* \leq 60$, we find $r \sim \mathcal{O}(10^{-3})$ in the limit $\xi_\phi \gg 1$, and $H_* \leq 3.4 \times 10^{-5} M_{\rm pl}$ for $\lambda_\phi/\xi_\phi^2 \leq 1.4 \times 10^{-8}$. In models like Higgs inflation [48], one typically finds $\lambda_\phi \sim \mathcal{O}(10^{-2}$–$10^{-4})$ at the energy scales of inflation (the range stemming from uncertainty in the value of the top-quark mass, which affects the running of λ_ϕ under renormalization-group flow) [95–97]. The range of λ_ϕ, in turn, requires $\xi_\phi \sim \mathcal{O}(10^2$–$10^3)$ at high energies—a reasonable range, given that ξ_ϕ typically rises with energy scale under renormalization-group flow with no UV fixed point [38]. Even for such large values of ξ_I, the inflationary dynamics occur at energy scales well below any nontrivial unitarity cutoff scale. (See Ref. [47] and references therein for further discussion.)

For the opposite limit, with $0 < \xi_\phi \ll 1$, a similar analysis yields [92,94]

$$H_* \simeq \sqrt{\frac{\lambda_\phi}{12\xi_\phi^2}\frac{\delta_*^4}{(1+\delta_*^2)^2}} M_{\rm pl}, \qquad N_* \simeq \frac{1}{8\xi_\phi}\delta_*^2,$$

$$\epsilon \simeq \frac{1}{N_*(1+8\xi_\phi N_*)}, \qquad (25)$$

where δ^2 is again defined as in Eq. (24). In this limit, the bound $r \leq 0.1$ requires $\xi_\phi \geq 0.006$ (for $N_* = 50$) or $\xi_\phi \geq 0.004$ (for $N_* = 60$), which in turn yields a constraint on λ_ϕ typical of minimally coupled models: $\lambda_\phi \sim \mathcal{O}(10^{-12})$ in order to keep $H_* \leq 3.4 \times 10^{-5} M_{\rm pl}$ [98,99]. Thus in the remainder of this analysis, we focus our attention on the range $10^{-3} \leq \xi_I \leq 10^4$.

A. Single-field attractor

Inflation begins in a regime in which $\xi_J(\phi^J)^2 > M_{\rm pl}^2$ for at least one component, J. The potential in the Einstein frame becomes asymptotically flat along each direction of field space, as each field ϕ^I becomes arbitrarily large:

$$V(\phi^I) \to \frac{M_{\rm pl}^4}{4}\frac{\lambda_I}{\xi_I^2}\left[1 + \mathcal{O}\left(\frac{M_{\rm pl}^2}{\xi_I(\phi^I)^2}\right)\right] \qquad (26)$$

(no sum on I). Unless some explicit symmetry constrains all coupling constants in the model to be identical ($\lambda_\phi = g = \lambda_\chi$, $\xi_\phi = \xi_\chi$), then the potential in the Einstein frame will develop ridges and valleys. Both the ridges and the valleys satisfy $V > 0$, and hence the system will inflate (albeit at different rates) whether the fields evolve along a ridge or a valley toward the global minimum of the potential. As seen in Fig. 1, even in the case of $\xi_I \ll 1$, in which inflation can occur for field values ϕ^I for which the potential has not reached its asymptotically flat form,
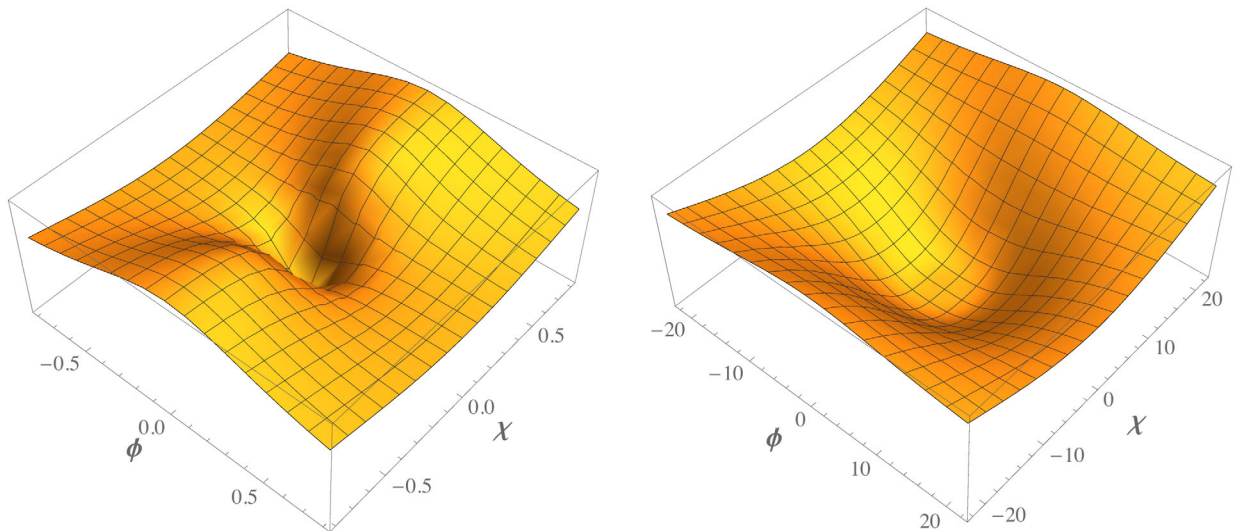

FIG. 1.   Potential in the Einstein frame, $V(\phi^I)$, for a two-field model with $\xi_\chi/\xi_\phi = 0.8$, $\lambda_\chi/\lambda_\phi = 1.25$, and $g/\lambda_\phi = 1$, for $\xi_\phi = 10^2$ (left) and $\xi_\phi = 10^{-2}$ (right). Field values are in units of $M_{\rm pl}$.
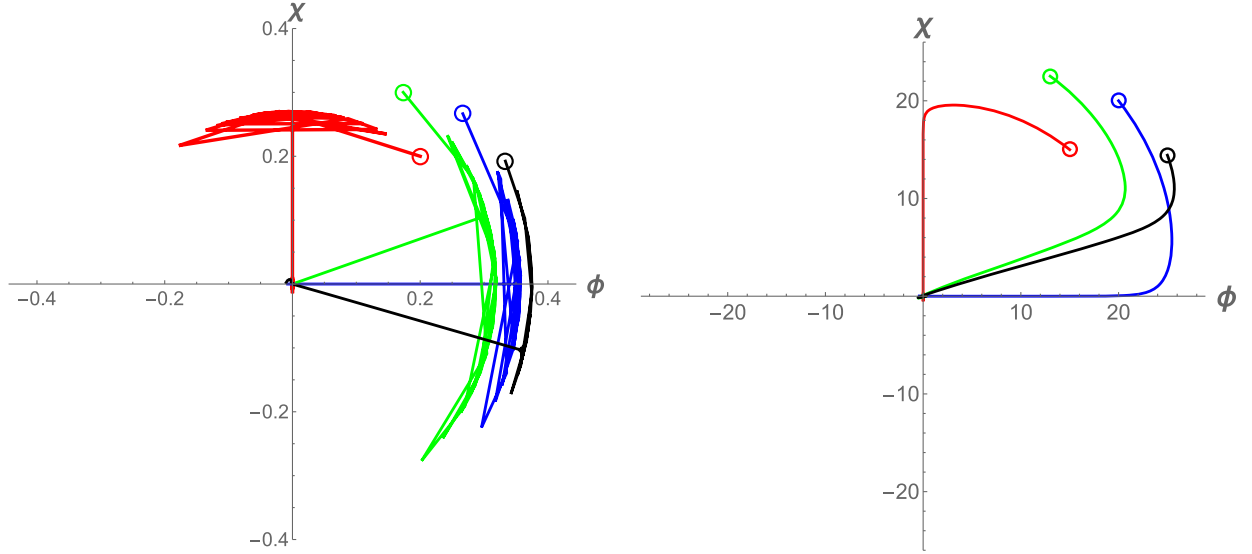
FIG. 2. Field trajectories for different couplings and initial conditions. Open circles indicate fields' initial values (in units of $M_{\rm pl}$). We set the fields' initial velocities to zero and vary the initial angle in field space, $\theta_0 \equiv \arctan(\chi_0/\phi_0)$. For the figure on the left, we set $\xi_\phi = 10^3$ and $\lambda_\phi = 10^{-2}$; for the figure on the right, we set $\xi_\phi = 10^{-1}$ and $\lambda_\phi = 10^{-10}$. In both figures, the other parameters $\{\xi_\chi, \lambda_\chi, g, \theta_0\}$ are $\{1.2\xi_\phi, 0.75\lambda_\phi, \lambda_\phi, \pi/4\}$ (red); $\{0.8\xi_\phi, \lambda_\phi, \lambda_\phi, \pi/4\}$ (blue); $\{0.8\xi_\phi, \lambda_\phi, 0.75\lambda_\phi, \pi/3\}$ (green); $\{0.8\xi_\phi, 1.2\lambda_\phi, 0.75\lambda_\phi, \pi/6\}$ (black). In each case, the initial transient motion damps out within a few efolds, yielding effectively single-field evolution for (at least) the final 65 efolds of inflation. Moreover, as demonstrated in Refs. [45,46], large field velocities at the start of inflation redshift away very quickly and do not significantly alter the single-field attractor behavior during inflation. Such large initial field velocities therefore have no impact on conditions at the start of preheating.

the potential still exhibits ridges and valleys, all of which are capable of supporting inflation.

Given the distinct ridge-valley structure of the effective potential in the Einstein frame, these models display strong single-field attractor behavior during inflation, across a wide range of couplings and initial conditions [46]. If the fields happen to begin evolving along the top of a ridge, they will eventually fall into a neighboring valley at a rate that depends on the local curvature of the potential [44,47]. Once the fields fall into a valley, Hubble drag quickly damps out any transverse motions in field space within a few efolds, after which the system evolves with virtually no turning in field space for the remainder of inflation [44–47]. As shown in Fig. 2, the single-field attractor behavior is as generic in the limit $\xi_I < 1$ as it is for $\xi_I \gg 1$. For all of the trajectories shown, the fields settle into a single-field attractor prior to the last 65 efolds of inflation.

Within a single-field attractor, these models predict values for spectral observables such as the primordial spectral index and its running (n_s and α), the ratio of power in tensor-to-scalar modes (r), primordial non-Gaussianity ($f_{\rm NL}$), and the fraction of power in isocurvature rather than adiabatic scalar modes ($\beta_{\rm iso}$) all in excellent agreement with the latest observations [44–47]. Figure 3 shows the tensor-to-scalar ratio r and the isocurvature fraction $\beta_{\rm iso}$ as a function of the nonminimal coupling. The approach to a constant ξ_I-independent value for large ξ_I is evident. The fields will only fail to settle into a single-field

attractor during inflation if *both* the ratios of certain coupling constants *and* the fields' initial conditions are fine-tuned. If the fields happen to begin very close to the top of a ridge, for example, and if the local curvature of the potential in the vicinity of that ridge has been fine-tuned to be small ($\mathcal{D}_{IJ}V/H^2 \ll 1$), then the system can exhibit significant turning in field space late in inflation [44,46,47]. In such fine-tuned cases, the system's evolution during the last 65 efolds of inflation can amplify non-Gaussianities and isocurvature perturbations, which could potentially be observable [44,47,86].

In Ref. [47] we analyzed the geometric structure of the attractor in the limit $\xi_I \gg 1$; here we generalize that analysis for arbitrary positive ξ_I. As in Ref. [47], we define convenient combinations of couplings,

$$\Lambda_\phi \equiv \lambda_\phi \xi_\chi - g\xi_\phi, \qquad \Lambda_\chi \equiv \lambda_\chi \xi_\phi - g\xi_\chi, \qquad \varepsilon \equiv \frac{\xi_\phi - \xi_\chi}{\xi_\phi},$$

$$(27)$$

along with the new rescaled quantities

$$\tilde{\Lambda}_\phi \equiv \frac{\Lambda_\phi}{\lambda_\phi \xi_\phi} = \frac{\xi_\chi}{\xi_\phi} - \frac{g}{\lambda_\phi}, \qquad \tilde{\Lambda}_\chi \equiv \frac{\Lambda_\chi}{\lambda_\chi \xi_\chi} = \frac{\xi_\phi}{\xi_\chi} - \frac{g}{\lambda_\chi}. \quad (28)$$
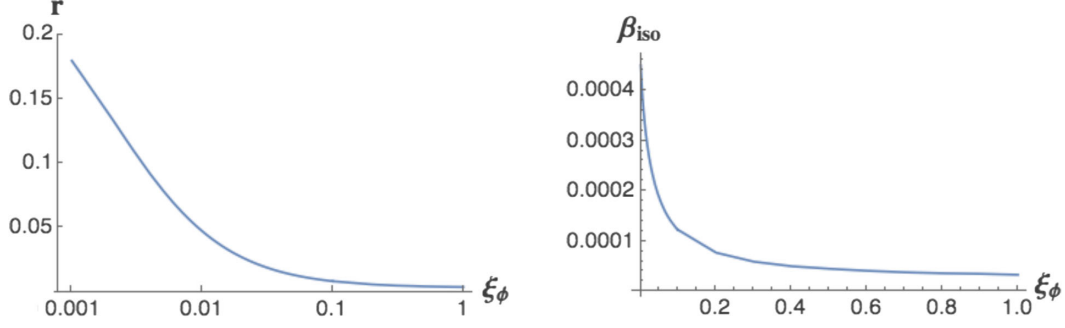
For arbitrary $\xi_I > 0$, we find

FIG. 3.　The tensor-to-scalar ratio (left) and the fraction of isocurvature modes (right) as a function of the nonminimal coupling ξ_ϕ. The isocurvature fraction is calculated for the symmetric (Higgs-like) case $\lambda_\phi = g = \lambda_\chi$ and $\xi_\phi = \xi_\chi$.

$$\mathcal{D}_{\chi\chi}V|_{\chi=0} = \frac{\lambda_\phi\phi^2}{[1+\delta^2]^3[1+(1+6\xi_\phi)\delta^2]}$$

$$\times \left[-\tilde{\Lambda}_\phi(1+6\xi_\phi)(\delta^2+\delta^4) \right.$$

$$\left. - (\tilde{\Lambda}_\phi + \varepsilon)\delta^2 + \frac{g}{\lambda_\phi} \right], \tag{29}$$

where $\delta^2 \equiv \xi_\phi\phi^2/M_{\rm pl}^2$ as in Eq. (24). In the limit $\xi_I \gg 1$, the quantity $\delta^2 \gg 1$ during inflation, and we find $\mathcal{D}_{\chi\chi}V|_{\chi=0} \propto -\Lambda_\phi$ [47]. In that limit, whenever $\Lambda_\phi < 0$ the direction $\chi = 0$ remains a local minimum of the potential and the background dynamics will obey strong attractor behavior along the direction $\chi = 0$. For $\xi_I \ll 1$, on the other hand, $\delta^2 \gtrsim 2$ during inflation, as may be seen from the scaling relationships in Eq. (25), and the orientation $\theta = \arctan(\chi/\phi)$ of the local minimum depends on the ellipticity, ε, and the ratio g/λ_ϕ in addition to the sign of Λ_ϕ. Even in these cases, the existence of attractor solutions remains generic (as shown in Fig. 2); only the orientation of the attractor in field space changes. For $\xi_I \ll 1$ there are special regions of parameter space for the coupling values where the topography of the potential can change during inflation, meaning that a ridge can turn into a valley as the inflaton rolls. Depending on the curvature, a waterfall-type transition may occur [100].

The orientation of the valley of the potential in field space, $\theta = \arctan(\chi/\phi)$, depends on combinations of couplings λ_I, g, and ξ_I [47]. When studying inflationary dynamics in multifield models, one typically projects physical quantities into adiabatic and isocurvature directions based on the motion of the background fields, φ^I [4,31,74–77,81]. For our two-field model, we may define the orthogonal unit vectors [44–47]

$$\hat{\sigma}^I \equiv \frac{\dot{\varphi}^I}{\dot{\sigma}}, \qquad \hat{s}^I \equiv \frac{\omega^I}{\omega} \tag{30}$$

in terms of the magnitude of the background fields' velocity, $\dot{\sigma}$, and their (covariant) turn rate,

$$\dot{\sigma} \equiv |\dot{\varphi}^I| = \sqrt{\mathcal{G}_{IJ}\dot{\varphi}^I\dot{\varphi}^J}, \qquad \omega^I \equiv \mathcal{D}_t\hat{\sigma}^I. \tag{31}$$

We may then project any field-space vector into adiabatic (σ) and isocurvature (s) components,

$$A_\sigma \equiv \hat{\sigma}_I A^I, \qquad A_s \equiv \hat{s}_I A^I. \tag{32}$$

Within a single-field attractor, $\omega^I \to 0$, so that a vector in field space that lies along the adiabatic direction at one time will continue to point along the adiabatic direction at later times. In that case, we may exploit the covariant nature of our framework to perform a rotation in field space, $\varphi^I \to \varphi^{I\prime}$, such that the valley of the potential lies along the direction $\chi' = 0$. Then the attractor will keep $\chi' \sim \dot{\chi}' \sim 0$, and only $\phi'(t)$ will evolve. With respect to the new field-space coordinates $\{\phi', \chi'\}$, the adiabatic direction points along ϕ' and the isocurvature direction along χ'.

We may quantify the strength of the attractor by examining the amount of fine-tuning needed to evade it. We will concentrate on the large-ξ_I regime, as it is enough to show the trend in the attractor's strength as a function of ξ_I. Following the analysis of Ref. [47] for the case where the fields φ^I start exponentially close to the top of a ridge, we use the linearized equations of motion to study the strength of the attractor. Apart from the fine-tuned curvature of the ridge ($\tilde{\Lambda}_\phi$), the dynamics of the inflaton field, which is translated into the attractor strength, depend very sensitively on the initial proximity to the top of the ridge. One obvious way to parametrize proximity to the top of the ridge is with the angle in field space, θ. The initial angle is $\theta_0 \approx \chi_0/\phi_0$ for $\chi_0 \ll \phi_0$. Our criterion will be the following: for the same dimensionless ridge curvature $\tilde{\Lambda}_\phi$ and the same initial proximity to the ridge θ_0, the strength of the attractor is defined through the number of efolds $N \leq 60$ it takes for the inflaton field to develop a large angle in field space, $\theta \simeq 1$.

Following the linearized analysis of Ref. [47], we take the dominant field ϕ to follow the single-field slow-roll solution, which is consistent to linear order in χ
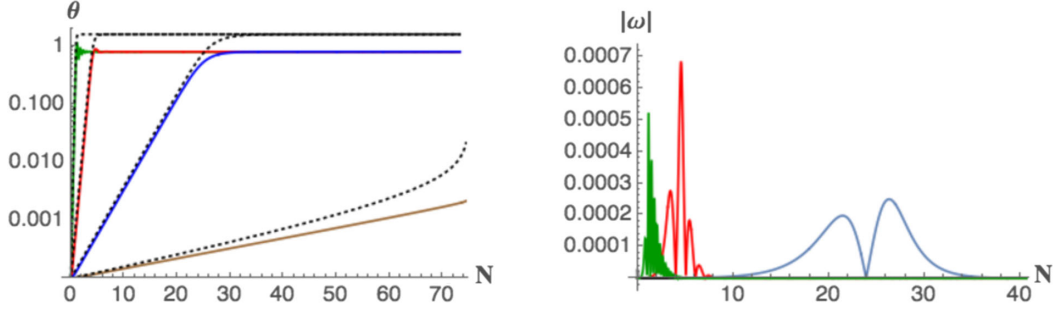
FIG. 4.　Left: evolution of the angle θ as a function of number of efolds from the beginning of inflation for $\tilde{\Lambda}_\phi = 0.001$, $\theta_0 = 10^{-4}$, $\xi_\chi = \xi_\phi$ and $\lambda_\phi = \lambda_\chi$. The values of the nonminimal coupling are $\xi_\phi = 10, 10^2, 10^3, 10^4$ (from bottom to top: brown, blue, red, and green, respectively). The black dotted lines show the analytic results from Eq. (38). Right: evolution of the turn rate $|\omega| \equiv |\omega^I|$ as a function of the number of efolds from the beginning of inflation for the same parameters and color coding. The turn rate for $\xi_\phi = 10$ is too small ($|\omega| \lesssim 10^{-7}$) to be visible on this plot.

$$\dot{\phi}_{\mathrm{SR}} = -\frac{\sqrt{\lambda_\phi} M_{\mathrm{pl}}^3}{3\sqrt{3}\xi_\phi^2 \phi}, \qquad (33)$$

which can be trivially solved to give

$$\phi = \sqrt{\phi_0^2 - \frac{4}{3}\frac{M_{\mathrm{pl}}^2}{\xi_\phi}N}, \qquad (34)$$

where $\phi(N = 0) = \phi_0$ at the start of inflation and we take the Hubble term to be constant during slow roll,

$$H \simeq \sqrt{\frac{\lambda_\phi}{12\xi_\phi^2}}M_{\mathrm{pl}}. \qquad (35)$$

The linearized equation of motion for the secondary field χ, when starting near the top of a smooth ridge ($\theta_0 \ll 1, \tilde{\Lambda}_\phi \ll 1$), is

$$\ddot{\chi} + 3H\dot{\chi} - \frac{\tilde{\Lambda}_\phi M_{\mathrm{pl}}^2}{\xi_\phi}\chi \simeq 0, \qquad (36)$$

and the solution (for $H = \text{constant}$) is

$$\chi(N) \simeq \chi_0 \exp\left[\left(-\frac{3}{2} + \sqrt{\frac{9}{4} + 12\tilde{\Lambda}_\phi \xi_\phi}\right)N\right]. \quad (37)$$

The evolution of the field-space angle θ follows immediately as

$$\theta(N) = \arctan\left(\theta_0 \frac{\exp\left[\left(-\frac{3}{2} + \sqrt{\frac{9}{4} + 12\tilde{\Lambda}_\phi \xi_\phi}\right)N\right]}{\sqrt{1 - \frac{4}{3}\frac{M_{\mathrm{pl}}^2}{\xi_\phi \phi_0^2}N}}\right). \qquad (38)$$

As we can easily see from Fig. 4, for the same amount of fine-tuning of the couplings $\tilde{\Lambda}_\phi$ and initial position θ_0, the

attractor gets stronger as ξ_ϕ increases. We only consider this fine-tuned regime, since for $\tilde{\Lambda} = \mathcal{O}(1)$ or $\theta_0 = \mathcal{O}(1)$, the approach to the attractor is too fast for the extraction of any reasonable conclusion. In Fig. 4 we also plot the turn rate $|\omega| \equiv |\omega^I|$ as a function of time. For $\xi_\phi = 10$ and fine-tuned initial conditions, the attractor is too weak and the field remains on the ridge for the duration of the inflationary epoch, leading to a suppressed turn rate $|\omega| \lesssim 10^{-7}$. For larger values of ξ_ϕ we see that the turn rate spikes at the time when $\theta \simeq 1$, as expected. The turn rate spikes earlier for larger couplings, indicating again a stronger attractor behavior. In the cases of $\xi_\phi = 10^3$, 10^4, the attractor is strong enough (meaning that the ridge is steep enough) that the field reaches the valley of the potential while having a significant velocity, which leads it to oscillate around the minimum before settling down to single-field motion. These oscillations perpendicular to the dominant motion of the inflaton can be seen as "primordial clocks" with possibly interesting observational consequences [101].

Equation (29) shows that for asymptotically large field values ($\delta \gg 1$) the ridge-valley nature of the potential is only defined by the sign of $\tilde{\Lambda}_\phi$, whereas after inflation has ended and the fields have settled into an oscillation pattern close to their minimum, in the limit of $\delta \lesssim 1$, the nature of the extremum is defined by the sign of g/λ_ϕ. There is of course a lot of parameter space between these two extremes, where for example the ellipticity ε can significantly affect the potential curvature. We will disentangle these effects one by one.

We start with the case of zero ellipticity, $\varepsilon = 0$, or $\xi_\phi = \xi_\chi$, which corresponds to $\tilde{\Lambda}_\phi = 1 - (g/\lambda_\phi)$. Figure 5 shows how the nature of the extremum at $\chi = 0$ varies with all relevant parameters, g/λ_ϕ, ξ_ϕ and ϕ. A field rolling along an attractor remains along this attractor throughout inflation and preheating. Furthermore, for $\xi_\phi \gtrsim 1$, the condition $g/\lambda_\phi > 1$ for the existence of an attractor remains quite accurate. For smaller ξ_ϕ, we see that even smaller
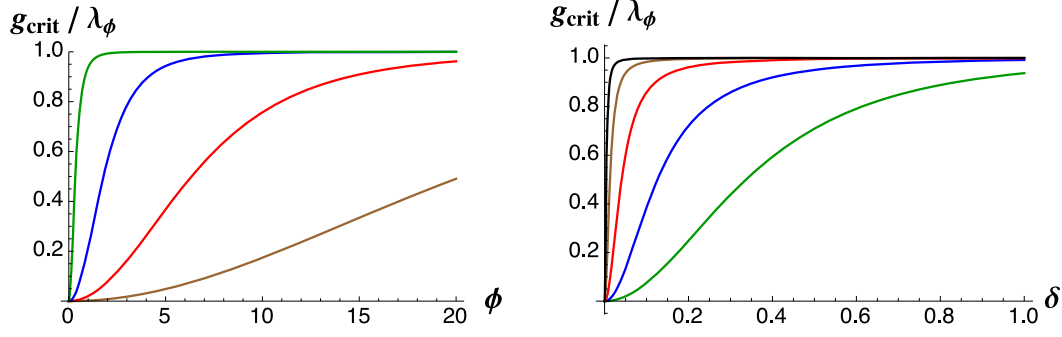
FIG. 5. Left: value of g/λ_ϕ for which $\mathcal{D}_{\chi\chi}V|_{\chi=0} = 0$ versus ϕ (in units of $M_{\rm pl}$) for $\xi_\phi = \xi_\chi$ and $\xi_\phi = 10^{-3}, 10^{-2}, 10^{-1}, 1$ (from bottom to top). Right: same quantity versus $\delta = \sqrt{\xi_\phi}\phi/M_{\rm pl}$ for $\xi_\phi = 1, 10, 100, 10^3, 10^4$ (from bottom to top). For values of g/λ_ϕ above each curve, the potential exhibits a valley along $\chi = 0$.

values of g/λ_ϕ can provide an attractor along $\chi = 0$. Even more interestingly, there are cases in which the extremum can change its nature during inflation. For example, for $\xi_\phi = 10^{-3}$ and $g/\lambda_\phi = 0.2$, we see that the direction $\chi = 0$ switches from a ridge to a valley around $\phi \approx 12$ (in units of $M_{\rm pl}$).

Next we consider the effect of an arbitrary ellipticity $\varepsilon \neq 0$. For simplicity, we choose two values of the ellipticity with opposite sign, $\varepsilon = 0.5$ and $\varepsilon = -1$, and compare them to the previous case $\varepsilon = 0$. The results are shown in Fig. 6. As expected, the values of g/λ_ϕ are shifted according to the ellipticity, since we can rewrite the parameter $\tilde{\Lambda}_\phi$ as

$$\tilde{\Lambda}_\phi = 1 - \varepsilon - \frac{g}{\lambda_\phi}. \qquad (39)$$

This means that in the limit where $\tilde{\Lambda}_\phi$ defines the nature of the extremum (for large δ), the extremum is a minimum for $g/\lambda_\phi > 1 - \varepsilon$. An interesting phenomenon occurs for positive ellipticity and $g/\lambda_\phi \gtrsim 1 - \varepsilon$. In this case, the critical value of g/λ_ϕ is a nonmonotonic function of ϕ. This means that for a value of g/λ_ϕ slightly above the

critical value, the valley, in which the field is rolling, can turn into a ridge and then into a valley again. This can trigger some genuinely multifield behavior, such as a waterfall transition, similar to hybrid inflation. Density perturbations during a waterfall transition require specialized treatment, due to the lack of a classical field trajectory around which to perturb, and can have interesting observational consequences such as seeding primordial black holes [100]. However, in the context of the family of models that we consider here, such waterfall transitions are rather fine-tuned cases, and we will not pursue them further.

In sum, these models include five coupling constants: λ_ϕ, λ_χ, g, ξ_ϕ, and ξ_χ. The Hubble scale during inflation is fixed by the combination $\lambda_\phi/\xi_\phi^2 \simeq 12H^2/M_{\rm Pl}^2$ (assuming the field is rolling along $\chi = 0$). We may reorganize the couplings in terms of the three nontrivial combinations Λ_ϕ, Λ_χ, ε, introduced in Eq. (27). Except for exponentially fine-tuned cases—fine-tuned in both parameter space and the fields' initial conditions—the predictions for cosmic microwave background (CMB) observables from these models follow the Starobinsky attractor for $\xi_\phi \gtrsim 10$ and essentially any values of the remaining parameter combinations, $\Lambda_\phi, \Lambda_\chi, \varepsilon$, as discussed in detail in Refs. [44,46,47].

Inflation ends when the scale factor stops accelerating, $\ddot{a}(t_{\rm end}) = 0$, which is equivalent to $\epsilon(t_{\rm end}) = 1$. (As a reminder, $\epsilon \equiv -\dot{H}/H^2$ should not be confused with the ellipticity parameter, $\varepsilon \equiv (\xi_\phi - \xi_\chi)/\xi_\phi$.) After $t_{\rm end}$, the background fields $\varphi^I(t)$ oscillate around the global minimum of the potential, governed by Eq. (15). If (as is generic) the system settles into the single-field attractor before the end of inflation, then the motion of $\varphi^I(t)$ in the direction of the potential's valley remains suppressed even after inflation. For example, if the system evolves along a valley in the $\chi = 0$ direction during inflation, then $\chi \sim \dot{\chi} \sim 0$ at $t_{\rm end}$ and Eq. (15) will maintain $\chi \sim \dot{\chi} \sim 0$ for times $t > t_{\rm end}$, as shown in Fig. 7. Such attractor behavior after $t_{\rm end}$ persists for at least as long as backreaction from perturbations may be neglected, consistent with the linearized treatment of Eq. (10). Thus the strong attractor
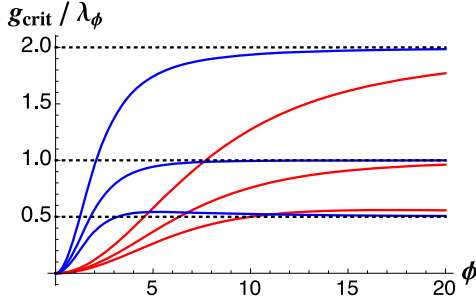

FIG. 6. The value of g/λ_ϕ for which $\mathcal{D}_{\chi\chi}V|_{\chi=0} = 0$ versus ϕ (in units of $M_{\rm pl}$) for $\xi_\phi = 10^{-1}$ (blue) and $\xi_\phi = 10^{-2}$ (red). For each value of ξ_ϕ, the ellipticity varies as $\varepsilon = -0.5, 1, 2$ (from top to bottom). For values of g/λ_ϕ above each curve, the potential exhibits a valley along $\chi = 0$.
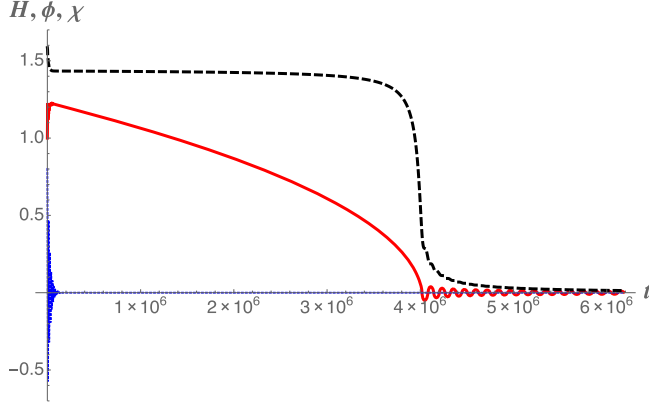
FIG. 7. The evolution of $H(t)$ (black dashed line), $\phi(t)$ (red solid line), and $\chi(t)$ (blue dotted line) during and after inflation, in units of $M_{\rm pl}$. The evolution shown here is for $\xi_\chi = 0.8\xi_\phi$, $\lambda_\chi = 1.25\lambda_\phi$, and $g = \lambda_\phi$, with $\xi_\phi = 10^2$, $\lambda_\phi = 10^{-4}$, and initial conditions $\phi(t_0) = 1$, $\chi(t_0) = 0.8$, $\dot{\phi}(t_0) = \dot{\chi}(t_0) = 0$. (We plot $5 \times 10^4 H$ so its magnitude is comparable to ϕ.) With these parameters and initial conditions, inflation lasts for $N_{\rm tot} = 111.6$ efolds until $t_{\rm end} = 3.99 \times 10^6$. The system rapidly falls into a valley along $\chi = 0$ within the first 3 efolds of inflation, after which $\chi(t)$ remains fixed at $\chi \sim 0$. After $t_{\rm end}$, $\phi(t)$ oscillates around the global minimum of the potential.

behavior that was identified in Refs. [44–47] is characteristic of the preheating phase as well.

The persistence of the attractor behavior after the end of inflation has important implications for preheating. In particular, although the unit vectors $\hat{\sigma}^I$ and $\hat{s}^I$ may become ill defined when the motion of $\varphi^I(t)$ is no longer monotonic, the orientation of the attractor in field space, $\theta = \arctan(\chi/\phi)$, remains unchanged after inflation. Upon performing a rotation $\varphi^I \to \varphi^{I\prime}$ such that $\chi' = 0$ lies along the direction of the attractor, then only one field, $\phi'(t)$, oscillates after $t_{\rm end}$. With only one background field oscillating, there is no "dephasing" of the background fields' oscillations, as is typical for multifield models with minimal couplings [24,66,67]. As shown in Refs. [1,2], these attractor models therefore predict robust, resonant amplification of fluctuations across wide regions of parameter space.

Within a single-field attractor, both the field-space metric, $\mathcal{G}_{IJ}$, and the mass-squared tensor, $\mathcal{M}_{IJ}$ of Eq. (18), become effectively diagonal. Upon rotating $\varphi^I \to \varphi^{I\prime}$ as needed so that the attractor lies along the direction $\chi' = 0$, then $\mathcal{G}_{\phi'\chi'} \sim \mathcal{G}^{\phi'\chi'} \sim 0$ and $\mathcal{M}^{\phi'}{}_{\chi'} \sim \mathcal{M}^{\chi'}{}_{\phi'} \sim 0$. As we will see in Sec. IV, this feature greatly simplifies the analysis of the fluctuations. Given that we may always perform such a field-space rotation, for most of the following analysis we restrict our attention to cases in which the attractor lies along the direction $\chi = 0$, with no loss of generality. In Sec. IV C we demonstrate that our results remain robust even for cases in which the attractor lies along some other direction θ in field space.

B. End of inflation and effective equation of state

Within the single-field attractor, we may readily study how $\phi(t_{\rm end})$ depends on the coupling constants. First we note that in the single-field attractor (assumed to lie along a $\chi = 0$ valley), the evolution of $\phi(t)$ becomes independent of λ_χ, g, and ξ_χ. Furthermore, we may rescale $t \to \tau \equiv \sqrt{\lambda_\phi} t$ without affecting the dynamics: $N = \int H dt = \int \mathcal{H} d\tau$ remains unchanged, as does $\epsilon = -\mathcal{H}'/\mathcal{H}^2 = -\dot{H}/H^2$ (where $\mathcal{H} \equiv a'/a$ and primes denote $d/d\tau$). Therefore $\phi(\tau_{\rm end}) = \phi(t_{\rm end})$. Thus in the single-field attractor, the value of ϕ at the end of inflation depends only on ξ_ϕ. In the limit $\xi_\phi \gg 1$, we expect inflation to end when $\xi_\phi \phi^2(t_{\rm end}) \simeq M_{\rm pl}^2$, which is indeed the behavior we observe. As shown in Fig. 8, $\phi(t_{\rm end})$ is very well fit by $\phi(t_{\rm end}) = 0.8 M_{\rm pl}/\sqrt{\xi_\phi}$ for $\xi_\phi \geq 1$, whereas $\phi(t_{\rm end}) \to 2.1 M_{\rm pl}$ in the limit $\xi_\phi \ll 1$, approaching the result of a minimally coupled ϕ^4 model. The value $\phi(t_{\rm end})$ sets the initial amplitude of oscillations at the start of preheating.

We may estimate the effective equation of state during the preheating phase by using the virial theorem [102]. The total kinetic energy for the system (to background order) is [44]

$$\frac{1}{2}\dot{\sigma}^2 \equiv \frac{1}{2}\mathcal{G}_{IJ}\dot{\varphi}^I\dot{\varphi}^J, \tag{40}$$

and the energy density and pressure are given by

$$\rho = \frac{1}{2}\dot{\sigma}^2 + V(\varphi^I),$$
$$p = \frac{1}{2}\dot{\sigma}^2 - V(\varphi^I). \tag{41}$$

If we assume an equation of state of the form $p = w\rho$, then we find

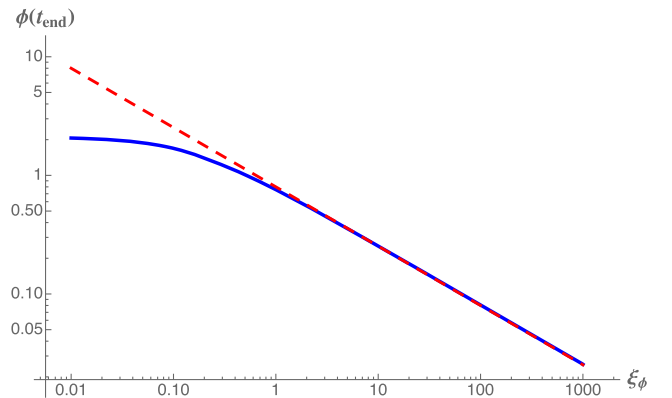$$w = \frac{\dot{\sigma}^2 - 2V}{\dot{\sigma}^2 + 2V} \tag{42}$$

FIG. 8. Within the single-field attractor, the value of $\phi(t_{\rm end})$ depends only on ξ_ϕ. The blue curve shows the numerical evaluation of $\phi(t_{\rm end})$ (in units of $M_{\rm pl}$), while the red dashed curve shows $0.8/\sqrt{\xi_\phi}$.

to background order. Using Eqs. (16), (40), and (41), we may rewrite Eq. (22) as $\epsilon = 3\dot{\sigma}^2/(\dot{\sigma}^2 + 2V)$. At $t_{\rm end}$, before the oscillations have begun, we have $\epsilon = 1$ and therefore $w = -1/3$, independent of couplings.

To estimate w once the background fields begin to oscillate, we define a covariant expression for the virial, q,

$$q \equiv \mathcal{G}_{IJ}\dot{\varphi}^I \varphi^J. \tag{43}$$

Upon using $\partial \mathcal{G}_{IJ}/\partial t = (\partial_K \mathcal{G}_{IJ})\dot{\varphi}^K$ and the usual relations among the Christoffel symbols $\Gamma^I{}_{JK}$, we find

$$\dot{q} = \dot{\sigma}^2 - V_{,J}\varphi^J + \frac{1}{2}(\partial_K \mathcal{G}_{IJ})\dot{\varphi}^I \dot{\varphi}^J \varphi^K. \tag{44}$$

Equation (44) is analogous to applications of the virial theorem in general relativity, in which corrections to the Newtonian result enter as gradients of the metric components [103]. For trajectories within the single-field attractor (with $\chi \sim \dot{\chi} \sim 0$), we have $\dot{\sigma}^2 \simeq \mathcal{G}_{\phi\phi}\dot{\phi}^2$ and Eq. (44) becomes

$$\dot{q} \simeq \dot{\sigma}^2\left[1 + \frac{1}{2}\phi\partial_\phi \ln \mathcal{G}_{\phi\phi}\right] - V_{,J}\varphi^J. \tag{45}$$

From Eqs. (4) and (20), we further find

$$V_{,J}\varphi^J = 2M_{\rm pl}^2 \frac{V}{f}, \tag{46}$$

where f is the nonminimal-coupling function of Eq. (19). Upon time averaging over several oscillations we have $\langle\dot{q}\rangle = 0$, and hence

$$\langle\dot{\sigma}^2\rangle + \frac{1}{2}\langle\dot{\sigma}^2 \cdot \phi\partial_\phi \ln \mathcal{G}_{\phi\phi}\rangle = 2M_{\rm pl}^2\langle V/f\rangle, \tag{47}$$

where the second term on the left-hand side is the contribution of the stretched field-space manifold. The equation of state can be calculated by noting that energy conservation requires (if one neglects Hubble friction)

$$\dot{\sigma}^2 + 2V = 2V_{\rm max}, \tag{48}$$

which allows Eq. (42) to be written solely in terms of ϕ and not $\dot{\phi}$.

After $t_{\rm end}$, $\phi(t)$ begins to oscillate with an initial amplitude $\phi(t_{\rm end}) \sim M_{\rm pl}/\sqrt{\xi_\phi}$ for $\xi_\phi \gtrsim 1$; at later times, its amplitude falls due to both the expansion of the Universe and the transfer of energy to decay products. Figure 9 shows the equation of state $w_{\rm avg}$ calculated by solving the background evolution and averaging Eq. (42) over several oscillations of $\phi(t)$, starting at the end of inflation, when $w = -1/3$. We see that for large nonminimal couplings, the equation of state spends more time around $w_{\rm avg} \approx 0$, as the
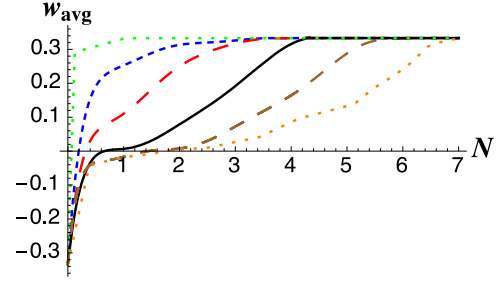

FIG. 9.   The equation of state, w from Eq. (42), averaged over several oscillations of $\phi(t)$, as a function of efolds, N, after the end of inflation. From bottom to top: $\xi_\phi = 10^4$ (orange dotted line), $\xi_\phi = 10^3$ (brown dashed line), $\xi_\phi = 10^2$ (black line), $\xi_\phi = 10$ (red dashed line), $\xi_\phi = 1$ (blue short-dashed line), and $\xi_\phi = 0.1$ (green dotted line). All simulations used $\xi_\chi = 0.8\xi_\phi$, $\lambda_\chi = 1.25\lambda_\phi$, and $g = \lambda_\phi$. Initial conditions at the start of inflation were set as $\theta_0 = \arctan(\chi_0/\phi_0) = \pi/6$; in each case, the fields settled into the single-field attractor along $\chi \sim 0$ before the end of inflation.

Universe continues to expand, while eventually reaching $w_{\rm avg} = 1/3$ at late times. Early in the oscillation phase, in other words, the conformal stretching of the Einstein-frame potential makes the background field behave more like a minimally coupled field in a quadratic potential, $V(\phi) = \frac{1}{2}m^2\phi^2$, than a quartic potential, $V(\phi) = \frac{\lambda}{4}\phi^4$. At late times, however, the system behaves like radiation, as in the minimally coupled case. Calculated to background order, $w_{\rm avg}$ reaches $1/3$ within several efolds after the end of inflation across the range $10^{-1} \leq \xi_\phi \leq 10^4$.

C. Background-field oscillations

To facilitate comparison with the well-studied case of a minimally coupled field with quartic self-coupling, in this subsection we neglect Hubble expansion during the oscillating phase. This approximation becomes more reliable as the frequency of oscillation ω grows significantly larger than H; in our case, we find a modest separation of time scales, with $\omega/H > 1$ across a wide range of ξ_ϕ. (One may incorporate effects from the expansion of the Universe perturbatively [104], though the $H \sim 0$ limit will suffice for our purposes here.)

Within the single-field attractor, in the limit $H \to 0$ and neglecting backreaction from produced particles, Eq. (15) becomes

$$\ddot{\phi} + \Gamma^\phi{}_{\phi\phi}\dot{\phi}^2 + \mathcal{G}^{\phi\phi}V_{,\phi} \simeq 0. \tag{49}$$

We rescale $\tau \equiv \sqrt{\lambda_\phi}t$, so that the dynamics depend only on ξ_ϕ. After $\tau_{\rm end}$, $\phi(\tau)$ oscillates periodically with period given by

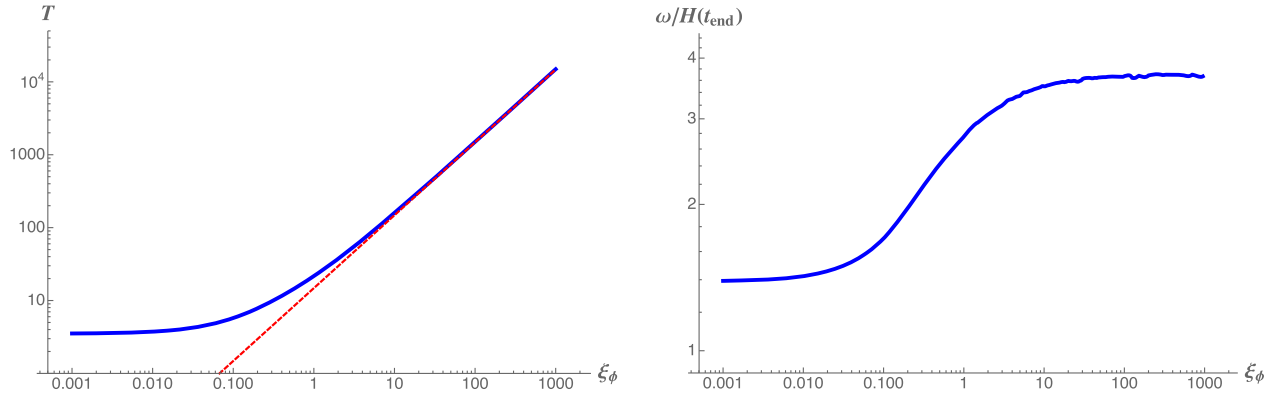$$T = 2\int_{-\phi_0}^{\phi_0} d\phi \sqrt{\frac{\mathcal{G}_{\phi\phi}}{2V(\phi_0) - 2V(\phi)}}. \tag{50}$$

FIG. 10.   Left: period of $\phi(\tau)$'s oscillations, T [in units of $(\sqrt{\lambda_\phi}M_{\rm pl})^{-1}$], as a function of ξ_ϕ, within the single-field attractor. For large ξ_ϕ, T grows linearly with ξ_ϕ, asymptoting to $T \to 14.8\xi_\phi/M_{\rm pl}$ (red dashed line). Right: ratio of the frequency of ϕ's oscillations, $\omega = 2\pi/T$, to the Hubble scale at the end of inflation, $H(t_{\rm end})$. For large ξ_ϕ, both ω and $H(t_{\rm end})$ scale as $1/\xi_\phi$, yielding $\omega/H(t_{\rm end}) \simeq 4$.

[In this subsection we label $\phi_0 = \phi(\tau_{\rm end})$ as the amplitude of the field at the start of preheating, rather than the start of inflation.] As shown in Fig. 10, the period scales approximately linearly with ξ_ϕ for $\xi_\phi > 1$, and hence the frequency of oscillations $\omega = 2\pi/T$ scales like $1/\xi_\phi$. The Hubble scale at the end of inflation $H(t_{\rm end})$ also scales like $1/\xi_\phi$ in the limit of large ξ_ϕ. We find $\omega/H(t_{\rm end}) > 1$ across the entire range $10^{-3} \leq \xi_\phi \leq 10^3$, with $\omega/H(t_{\rm end}) \sim 3$ at $\xi_\phi = 1$ and $\omega/H(t_{\rm end}) \to 4$ for $\xi_\phi \gg 1$.

In the limit $\xi_\phi \gg 1$, the integral for T in Eq. (50) may be calculated analytically. For initial data of the form $\phi_0 = \phi(\tau_{\rm end}) = \alpha M_{\rm pl}/\sqrt{\xi_\phi}$ for some constant α, and working in the regime $\alpha > 1/\sqrt{6\xi_\phi}$, we find

$$T \to \frac{4\sqrt{3}\xi_\phi}{M_{\rm pl}}\left[\pi - \arctan\left(\frac{\sqrt{1+2\alpha^2}}{\alpha^2}\right)\right]\frac{1+\alpha^2}{\sqrt{1+2\alpha^2}}. \quad (51)$$

Details of the derivation may be found in Appendix B. Using the best-fit value $\alpha = 0.8$ (see Fig. 8) yields $T \to 14.8\xi_\phi/M_{\rm pl}$ in the limit $\xi_\phi \gg 1$. Meanwhile, in the opposite limit, $\xi_\phi \to 0$, Eq. (49) may be solved analytically as a Jacobian elliptic cosine, given the Jordan-frame potential of Eq. (20): $\phi(t) = \phi_0{\rm cn}(\phi_0\tau, 1/\sqrt{2})$ [105–107]. The function ${\rm cn}(x, \kappa)$ is periodic with period $4K(\kappa)$, where $K(\kappa)$ is the complete elliptic integral of the first kind [108]. Given $\kappa = 1/\sqrt{2}$ and $\phi_0 = 2.1M_{\rm pl}$ for $\xi_\phi = 0$, we find $T \to 4K(1/\sqrt{2})/\phi_0 = 3.9/M_{\rm pl}$, a good match to the $\xi_\phi \ll 1$ behavior of Fig. 10.

More generally, the terms in Eq. (49) that arise from the nontrivial field-space metric produce a richer structure for ϕ's oscillations, with greater numbers of non-negligible harmonics, compared to the $\xi_\phi = 0$ case. In Ref. [1] we study this nontrivial harmonic structure and analyze its impact on the structure of the resonances for the coupled fluctuations.

IV. EVOLUTION OF THE FLUCTUATIONS

In order to study the evolution of the fluctuations Q^I during preheating, we expand the action to second order in both field and metric perturbations, calculate the energy density, and perform a (covariant) mode expansion. These steps enable us to relate the number density of particles for each species to an adiabatic parameter, generalizing the usual single-field expression. The adiabatic parameters may be used to identify regions of parameter space in which the system departs strongly from adiabatic evolution, indicating explosive particle production. We identify important differences in the behavior of the system for three distinct regimes: $\xi_I < \mathcal{O}(1)$, $\xi_I \sim \mathcal{O}(1-10)$, and $\xi_I \geq \mathcal{O}(100)$, which we explore further in Refs. [1,2]. These three regimes correspond to what one might expect, *a priori*, on perturbative grounds: $\xi_I \to 0$ (semiclassical analysis), $\xi_I \sim 1$ (nontrivial quantum corrections), and $\xi_I \to \infty$ (nonperturbative regime).

A. Mode expansion and adiabatic parameters

Following the method of Ref. [82] applied to the action in Eq. (3), we may expand the action to second order in the doubly covariant fluctuation Q^I. We find (see also Refs. [44,80,86])

$$S_2^{(Q)} = \int d^3x \, dt \, a^3(t) \left[-\frac{1}{2}\bar{g}^{\mu\nu}\mathcal{G}_{IJ}\mathcal{D}_\mu Q^I \mathcal{D}_\nu Q^J \right.$$
$$\left. -\frac{1}{2}\mathcal{M}_{IJ}Q^I Q^J\right], \quad (52)$$

where $\bar{g}_{\mu\nu}$ is the background spacetime metric, $\mathcal{M}_{IJ}$ is given in Eq. (18), and $\mathcal{G}_{IJ}$ and $\mathcal{M}_{IJ}$ are evaluated to background order in the fields, φ^I. Next we rescale the fluctuations, $Q^I(x^\mu) \to X^I(x^\mu)/a(t)$ and introduce conformal time, $d\eta = dt/a(t)$, so that the background spacetime line element may be written $ds^2 = a^2(\eta)\eta_{\mu\nu}dx^\mu dx^\nu$, in

terms of the Minkowski spacetime metric $\eta_{\mu\nu}$. Upon integrating by parts, we may rewrite Eq. (52) in the form

$$S_2^{(X)} = \int d^3x d\eta \left[-\frac{1}{2}\eta^{\mu\nu}\mathcal{G}_{IJ}\mathcal{D}_\mu X^I \mathcal{D}_\nu X^J - \frac{1}{2}\mathbb{M}_{IJ}X^I X^J \right]$$

(53)

where

$$\mathbb{M}_{IJ} \equiv a^2 \left(\mathcal{M}_{IJ} - \frac{1}{6}\mathcal{G}_{IJ}R \right)$$

(54)

and R is the spacetime Ricci scalar. We have used the relation $R = 6a''/a^3$, and in this section we will use primes to denote $d/d\eta$. Note that for an equation of state $w_{\text{avg}} \simeq 0$ then $a(t) \sim t^{2/3}$ and $a(\eta) \sim \eta^2$, while for $w_{\text{avg}} = 1/3$ then $a(t) \sim t^{1/2}$ and $a(\eta) \sim \eta$.

From Eq. (53) we may construct an energy-momentum tensor for the fluctuations,

$$T_{\mu\nu}^{(X)} = \mathcal{G}_{IJ}\mathcal{D}_\mu X^I \mathcal{D}_\nu X^J - \frac{1}{2}\eta_{\mu\nu}[\eta^{\alpha\beta}\mathcal{G}_{IJ}\mathcal{D}_\alpha X^I \mathcal{D}_\beta X^J + \mathbb{M}_{IJ}X^I X^J].$$

(55)

The energy density is given by the 00 component of $T_{\mu\nu}^{(X)}$. The background spacetime metric is spatially flat, so we may easily perform a Fourier transform of a given quantity, $F(x^\mu) = (2\pi)^{-3/2}\int d^3 k F_k(\eta)e^{i\mathbf{k}\cdot\mathbf{x}}$. The energy density of the fluctuations per Fourier mode then takes the form

$$\rho_k^{(X)} = \frac{1}{2}\mathcal{G}_{IJ}\mathcal{D}_\eta X_k^I \mathcal{D}_\eta X_k^J + \frac{1}{2}[\omega_k^2(\eta)]_{IJ}X_k^I X_k^J + \mathcal{O}(X^3),$$

(56)

where we have defined

$$[\omega_k^2(\eta)]_{IJ} \equiv k^2 \mathcal{G}_{IJ} + \mathbb{M}_{IJ}.$$

(57)

Upon using the equation of motion for Q^I, Eq. (17), and the relation $Q^I = X^I/a$, we may rewrite Eq. (56) in the form

$$\rho_k^{(X)} = \frac{1}{2}\mathcal{G}_{IJ}[(\mathcal{D}_\eta X^I)(\mathcal{D}_\eta X^J) - (\mathcal{D}_\eta^2 X^I)X^J].$$

(58)

Next we quantize the fluctuations, $X^I \to \hat{X}^I$, and expand them in a series of creation and annihilation operators in a way that respects the nontrivial field-space manifold [24,109],

$$\hat{X}^I(x^\mu) = \int \frac{d^3 k}{(2\pi)^{3/2}}$$
$$\times \sum_b [u_b^I(k,\eta)\hat{a}_{\mathbf{k}b}e^{i\mathbf{k}\cdot\mathbf{x}} + u_b^{I*}(k,\eta)\hat{a}_{\mathbf{k}b}^\dagger e^{-i\mathbf{k}\cdot\mathbf{x}}],$$

(59)

where the index $b = 1, 2, \ldots, N$. The operators obey

$$\hat{a}_{\mathbf{k}b}|0\rangle = 0, \qquad \langle 0|\hat{a}_{\mathbf{k}b}^\dagger = 0$$

(60)

for all $\mathbf{k}$ and b, and

$$[\hat{a}_{\mathbf{k}b}, \hat{a}_{\mathbf{q}c}] = [\hat{a}_{\mathbf{k}b}^\dagger, \hat{a}_{\mathbf{q}c}^\dagger] = 0,$$
$$[\hat{a}_{\mathbf{k}b}, \hat{a}_{\mathbf{q}c}^\dagger] = \delta^{(3)}(\mathbf{k} - \mathbf{q})\delta_{bc}.$$

(61)

Each of the mode functions satisfies the equation of motion,

$$\mathcal{D}_\eta^2 u_b^I + [\omega_k^2(\eta)]^I{}_J u_b^J = 0.$$

(62)

As discussed in Ref. [24], we have N linear, second-order differential equations (one for each $\hat{X}^I$), which yield $2N$ linearly independent solutions. By parametrizing the fluctuations as in Eq. (59), we have introduced N^2 complex mode functions $u_b{}^I(k,\eta)$, and hence $2N^2$ real-valued scalar functions, $u_b^I = \text{Re}[u_b^I] + \text{Im}[u_b^I]$. But N-tuples of the complex mode functions are coupled to each other by Eq. (62), which yields $2N(N-1)$ constraints, leaving exactly $2N^2 - 2N(N-1) = 2N$ independent solutions.

We parametrize the mode functions as [24,109]

$$u_b^I(k,\eta) = h_{(b,I)}(k,\eta)e_b^I(\eta),$$

(63)

where the $h_{(b,I)}$ are complex scalar functions and the $e_b^I(\eta)$ are vielbeins of the field-space metric,

$$\delta^{bc}e_b^I(\eta)e_c^J(\eta) = \mathcal{G}^{IJ}(\eta).$$

(64)

Note that the components of the vielbeins are purely real, and, unlike the unit vectors $\hat{\sigma}^I, \hat{s}^I$ defined in Eq. (30), the e_b^I are well behaved during preheating. (Explicit expressions for the e_b^I for our two-field model may be found in Appendix A.) The subscripts (b, I) on h are labels only, not vector indices. We then find

$$\langle 0|\hat{X}^I(x)\hat{X}^J(x)|0\rangle = \int \frac{d^3 k}{(2\pi)^3}\delta^{bc}u_b^I u_c^{J*},$$

(65)

upon using Eqs. (60), (61), and (64). As emphasized in Refs. [24,29], the cross products, with $I \neq J$, need not vanish.

The vielbeins "absorb" most of the added structure from the nontrivial field-space manifold, enabling us to manipulate (mostly) ordinary scalar functions. As usual, we raise and lower field-space indices I, J with $\mathcal{G}_{IJ}$, and we raise and lower internal indices b, c with δ_{bc}. We may also use the vielbeins to "trade" between field-space indices and internal indices. For an arbitrary vector A^I we may write

$$A^b = e^b{}_I A^I, \qquad A^I = e_b{}^I A^b,$$

(66)

while Eq. (64) implies

$$e^b{}_I e_c{}^I = \delta^b{}_c,$$
$$e_b{}^I e^b{}_J = \delta^I{}_J. \tag{67}$$

The covariant derivative of the vielbein with respect to $\mathcal{G}_{IJ}$ is given in terms of the spin connection, $\omega^{bc}{}_I$,

$$\mathcal{D}_I e^b{}_J = -\omega^{bc}{}_I e_{cJ}, \tag{68}$$

where $\omega^{bc}{}_I$ is antisymmetric in its internal indices, $\omega^{bc}{}_I = -\omega^{cb}{}_I$ [110]. Because of the antisymmetry of the spin connection, the (covariant) directional derivative with respect to conformal time vanishes,

$$\mathcal{D}_\eta e^b{}_J = 0 \tag{69}$$

for all b and J [109].

For our two-field model, with $\{I, J\} = \{1, 2\}$, we may write out the mode expansions more explicitly. We assign the field-space indices $1 = \phi$ and $2 = \chi$ and write $\hat{a}_{\mathbf{k}b} = \hat{b}_{\mathbf{k}}$ for $b = 1$, $\hat{a}_{\mathbf{k}b} = \hat{c}_{\mathbf{k}}$ for $b = 2$. We also label $h_{(1,\phi)} = v_k(\eta)$, $h_{(2,\phi)} = w_k(\eta)$, $h_{(1,\chi)} = y_k(\eta)$, and $h_{(2,\chi)} = z_k(\eta)$, so that Eq. (59) becomes

$$\hat{X}^\phi(x^\mu) = \int \frac{d^3k}{(2\pi)^{3/2}} [(v_k e_1{}^\phi \hat{b}_{\mathbf{k}} + w_k e_2{}^\phi \hat{c}_{\mathbf{k}}) e^{i\mathbf{k}\cdot\mathbf{x}}$$
$$+ (v_k^* e_1{}^\phi \hat{b}_{\mathbf{k}}^\dagger + w_k^* e_2{}^\phi \hat{c}_{\mathbf{k}}^\dagger) e^{-i\mathbf{k}\cdot\mathbf{x}}],$$
$$\hat{X}^\chi(x^\mu) = \int \frac{d^3k}{(2\pi)^{3/2}} [(y_k e_1{}^\chi \hat{b}_{\mathbf{k}} + z_k e_2{}^\chi \hat{c}_{\mathbf{k}}) e^{i\mathbf{k}\cdot\mathbf{x}}$$
$$+ (y_k^* e_1{}^\chi \hat{b}_{\mathbf{k}}^\dagger + z_k^* e_2{}^\chi \hat{c}_{\mathbf{k}}^\dagger) e^{-i\mathbf{k}\cdot\mathbf{x}}]. \tag{70}$$

Equation (62) couples v_k with y_k and w_k with z_k:

$$(v_k'' + \Omega^2_{(\phi)} v_k) e_1^\phi = -a^2 \mathcal{M}^\phi{}_\chi y_k e_1^\chi,$$
$$(w_k'' + \Omega^2_{(\phi)} w_k) e_2^\phi = -a^2 \mathcal{M}^\phi{}_\chi z_k e_2^\chi,$$
$$(y_k'' + \Omega^2_{(\chi)} y_k) e_1^\chi = -a^2 \mathcal{M}^\chi{}_\phi v_k e_1^\phi,$$
$$(z_k'' + \Omega^2_{(\chi)} z_k) e_2^\chi = -a^2 \mathcal{M}^\chi{}_\phi w_k e_2^\phi, \tag{71}$$

where for convenience we have labeled the diagonal components of $[\omega_k^2(\eta)]^I{}_J$ as

$$\Omega^2_{(\phi)}(k, \eta) \equiv k^2 + a^2 m^2_{\text{eff},\phi}(\eta),$$
$$\Omega^2_{(\chi)}(k, \eta) \equiv k^2 + a^2 m^2_{\text{eff}\chi}(\eta), \tag{72}$$

in terms of the effective masses

$$m^2_{\text{eff},\phi} \equiv \mathcal{M}^\phi{}_\phi - \frac{1}{6}R,$$
$$m^2_{\text{eff},\chi} \equiv \mathcal{M}^\chi{}_\chi - \frac{1}{6}R. \tag{73}$$

We are interested in the energy density per mode k of the quantized fluctuations, which we parametrize as

$$\langle \hat{\rho}^{(X)}(x^\mu) \rangle = \int \frac{d^3k}{(2\pi)^3} \rho_k^{(X)\text{vev}}(\eta). \tag{74}$$

Upon using Eqs. (58), (65), and (69) we find

$$\rho_k^{(X)\text{vev}} = \frac{1}{2} \mathcal{G}_{IJ} \sum_b \sum_c \{\delta^{bc}[h'_{(b,I)} h^{*\prime}_{(c,J)} - h''_{(b,I)} h^*_{(c,J)}] e_b{}^I e_c{}^J\}$$
$$= \rho_k^{(\phi)} + \rho_k^{(\chi)} + \rho_k^{(\text{int})}, \tag{75}$$

with

$$\rho_k^{(\phi)} = \frac{1}{2} \mathcal{G}_{\phi\phi} \{(|v_k'|^2 - v_k'' v_k^*) e_1^\phi e_1^\phi + (|w_k'|^2 - w_k'' w_k^*) e_2^\phi e_2^\phi\},$$
$$\rho_k^{(\chi)} = \frac{1}{2} \mathcal{G}_{\chi\chi} \{(|y_k'|^2 - y_k'' y_k^*) e_1^\chi e_1^\chi + (|z_k'|^2 - z_k'' z_k^*) e_2^\chi e_2^\chi\},$$
$$\rho_k^{(\text{int})} = \mathcal{G}_{\phi\chi} \{(v_k' y_k^{*\prime} - v_k'' y_k^*) e_1^\phi e_1^\chi + (y_k' v_k^{*\prime} - y_k'' v_k^*) e_1^\chi e_1^\phi$$
$$+ (w_k' z_k^{*\prime} - w_k'' z_k^*) e_2^\phi e_2^\chi + (z_k' w_k^{*\prime} - z_k'' w_k^*) e_2^\chi e_2^\phi\}. \tag{76}$$

One may use the equations of motion in Eq. (71) to demonstrate that the expressions in Eq. (76) are purely real. The number density per mode of quanta of a given field I (ϕ or χ) may be related to the energy density by

$$n_k^{(I)} = \frac{\rho_k^{(I)}}{\Omega_{(I)}} - \frac{1}{2}. \tag{77}$$

The number density per mode for each species $I = \phi, \chi$ will be well defined in the limit $\rho_k^{(\text{int})} \ll \rho_k^{(I)}$.

We noted in Sec. III A that within a single-field attractor (along the direction $\chi = 0$), the cross-terms in both $\mathcal{G}_{IJ}$ and $\mathcal{M}^I{}_J$ vanish. In that case, the vielbeins also become diagonal,

$$e_b^I \to \begin{pmatrix} e_1^\phi & 0 \\ 0 & e_2^\chi \end{pmatrix}, \tag{78}$$

with $e_2^\phi \sim e_1^\chi \sim 0$, $e_1^\phi e_1^\phi \simeq \mathcal{G}^{\phi\phi}$, $e_2^\chi e_2^\chi \simeq \mathcal{G}^{\chi\chi}$, and $\mathcal{G}_{\phi\phi}\mathcal{G}^{\phi\phi} = \mathcal{G}_{\chi\chi}\mathcal{G}^{\chi\chi} = 1 + \mathcal{O}(\chi^2)$. Then the fluctuations $\hat{X}^I$ simplify considerably: $\hat{X}^\phi$ is expanded only in the $\hat{b}_{\mathbf{k}}, \hat{b}_{\mathbf{k}}^\dagger$ operators, and $\hat{X}^\chi$ only in the $\hat{c}_{\mathbf{k}}, \hat{c}_{\mathbf{k}}^\dagger$ operators. Given both $\mathcal{M}^\phi{}_\chi \sim \mathcal{M}^\chi{}_\phi \sim 0$ and $e_2^\phi \sim e_1^\chi \sim 0$, moreover, the scalar mode functions decouple: the functions $v_k(\eta)$ and $z_k(\eta)$

satisfy source-free equations of motion, while $w_k(\eta) \sim y_k(\eta) \sim 0$. Within the attractor, the expressions in Eq. (76) simplify as well:

$$\rho_k^{(\phi)} \to \frac{1}{2}(|v_k'|^2 - v_k'' v_k^*) + \mathcal{O}(\chi^2),$$
$$\rho_k^{(\chi)} \to \frac{1}{2}(|z_k'|^2 - z_k'' z_k^*) + \mathcal{O}(\chi^2),$$
$$\rho_k^{(\text{int})} \to \mathcal{O}(\chi^2) \sim 0. \tag{79}$$

Since $\rho_k^{(\text{int})}$ remains subdominant within the single-field attractor, the notion of particle number for each species is well defined in that limit, and we may relate $\rho_k^{(\phi)}$ and $\rho_k^{(\chi)}$ to the corresponding number densities of produced particles.

To calculate the number density of created particles and relate those expressions to adiabatic parameters, we generalize the familiar result from studies of single-field models with minimal couplings. (See also Refs. [66, 111–113].) Within the single-field attractor, the coupled equations of motion in Eq. (71) reduce to

$$v_k'' + \Omega_{(\phi)}^2(k,\eta) v_k \simeq 0,$$
$$z_k'' + \Omega_{(\chi)}^2(k,\eta) z_k \simeq 0. \tag{80}$$

We are interested in how efficiently the background fields φ^I transfer energy to the fluctuations after the end of inflation, so we quantize the fluctuations with respect to the adiabatic vacuum $|0(t_{\text{end}})\rangle$, that is, the state that instantaneously minimizes the system's energy density at t_{end} [24,37,39]. We then posit solutions to Eq. (80) of the form

$$v_k(\eta) = \frac{1}{\sqrt{2W_{(\phi)}(k,\eta)}} \exp\left[-i \int^\eta d\eta' W_{(\phi)}(k,\eta')\right],$$
$$z_k(\eta) = \frac{1}{\sqrt{2W_{(\chi)}(k,\eta)}} \exp\left[-i \int^\eta d\eta' W_{(\chi)}(k,\eta')\right], \tag{81}$$

in terms of the (as yet unspecified) real-valued functions $W_{(I)}(k,\eta)$. The choice of adiabatic vacuum corresponds to the boundary conditions $W_{(\phi)}(k,\eta_{\text{end}}) = \Omega_{(\phi)}(k,\eta_{\text{end}})$ and $W_{(\chi)}(k,\eta_{\text{end}}) = \Omega_{(\chi)}(k,\eta_{\text{end}})$. Given the ansatz in Eq. (81), the expressions in Eq. (76) for the energy density per mode take the form

$$\rho_k^{(\phi)} = \frac{1}{2}\left[W_{(\phi)} + \frac{W_{(\phi)}''}{4W_{(\phi)}^2} - \frac{W_{(\phi)}'^2}{4W_{(\phi)}^3}\right] + \mathcal{O}(\chi^2), \tag{82}$$

and likewise for $\rho_k^{(\chi)}$ in terms of $W_{(\chi)}$ and its derivatives.

Within the single-field attractor, when $\rho_k^{(\text{int})} \sim 0$ and $\rho_k^{(\phi)}$ and $\rho_k^{(\chi)}$ assume the simple forms in Eq. (79), the number densities in Eq. (77) likewise simplify. We may also use Eq. (80) to relate $W_{(\phi)}(k,\eta)$ to $\Omega_{(\phi)}(k,\eta)$, which yields

$$W_{(\phi)}^2 = \Omega_{(\phi)}^2 - \frac{1}{2}\left[\frac{W_{(\phi)}''}{W_{(\phi)}} - \frac{3}{2}\frac{W_{(\phi)}'}{W_{(\phi)}^2}\right]. \tag{83}$$

Away from resonance bands we expect the modes to evolve adiabatically, for which $W_{(\phi)}(k,\eta) \to \Omega_{(\phi)}(k,\eta) + \mathcal{O}(\mathcal{A}_{(\phi)}^2)$, where

$$\mathcal{A}_{(\phi)}(k,\eta) \equiv \frac{\Omega_{(\phi)}'(k,\eta)}{\Omega_{(\phi)}^2(k,\eta)}. \tag{84}$$

As in Ref. [37], we may then solve Eq. (83) iteratively, in increasing powers of $\mathcal{A}_{(\phi)}$. Combining Eqs. (82)–(84), we find

$$n_k^{(\phi)} = \frac{1}{16}\mathcal{A}_{(\phi)}^2 + \mathcal{O}(\chi^2) + \mathcal{O}(\mathcal{A}_{(\phi)}^3), \tag{85}$$

with a comparable expression for $n_k^{(\chi)}$. Much as in familiar cases with minimally coupled fields [24,66,111,112], regions of parameter space in which $\mathcal{A}_{(I)}(k,\eta) \gg 1$ correspond to strong departures from adiabatic evolution, and hence to bursts of particle production.

B. Resonant amplification within the attractor

The behavior of the adiabatic parameters, $\mathcal{A}_{(I)}(k,\eta)$, depends upon the effective frequencies, $\Omega_{(I)}(k,\eta)$, which in turn depend upon the effective masses, $m_{\text{eff},I}^2$, defined in Eq. (73). After the end of inflation, as $\varphi^I(t)$ oscillates, one or more of the $m_{\text{eff},I}^2$ will oscillate as well, which can drive resonant amplification of the coupled fluctuations, $\hat{Q}^I$. We may rewrite Eq. (84) in terms of cosmic time rather than conformal time,

$$\mathcal{A}_{(I)} = \frac{H^{-3}\partial_t m_{\text{eff},I}^2 + 2(m_{\text{eff},I}/H)^2}{2[\ell^2 + (m_{\text{eff},I}/H)^2]^{3/2}}, \tag{86}$$

where $\ell \equiv k_{\text{phys}}/H = k/(aH)$. In the limit $\ell \ll 1$, we find

$$\mathcal{A}_{(I)} = \frac{\partial_t m_{\text{eff},I}^2}{2m_{\text{eff},I}^3} + \frac{H}{m_{\text{eff},I}} + \mathcal{O}(\ell^2). \tag{87}$$

In the limit $k \ll aH$, we expect $|\mathcal{A}_{(I)}| \gg 1$ whenever $\partial_t m_{\text{eff},I}^2$ spikes and/or $m_{\text{eff},I}^2$ passes through zero.

Given the form of Eq. (73), we may distinguish four separate contributions to $m_{\text{eff},\phi}^2$:

$$m_{\text{eff},\phi}^2 = m_{1,\phi}^2 + m_{2,\phi}^2 + m_{3,\phi}^3 + m_{4,\phi}^2, \tag{88}$$

where

$$m_{1,\phi}^2 \equiv \mathcal{G}^{\phi K}(\mathcal{D}_\phi \mathcal{D}_K V),$$

$$m_{2,\phi}^2 \equiv -\mathcal{R}^\phi{}_{LM\phi}\dot{\varphi}^L\dot{\varphi}^M,$$

$$m_{3,\phi}^2 \equiv -\frac{1}{M_{\rm pl}^2 a^3}\delta^\phi{}_I\delta^J{}_\phi \mathcal{D}_t\left(\frac{a^3}{H}\dot{\varphi}^I\dot{\varphi}_J\right),$$

$$m_{4,\phi}^2 \equiv -\frac{1}{6}R, \tag{89}$$

with comparable expressions for the contributions to $m_{\rm eff,\chi}^2$. Note that $m_{1,I}^2$ arises from the gradient of the potential; $m_{2,I}^2$ from the nontrivial field-space manifold; $m_{3,I}^2$ from the coupled metric perturbations; and $m_{4,I}^2$ from the expansion of the background spacetime. The term $m_{2,I}^2$, in particular, has no analog in models with minimally coupled fields and canonical kinetic terms, and can play important roles in the dynamics during and after inflation [44–47,78–83,114,115].

We first note that

$$m_{4,I}^2 = -\frac{1}{6}R = -(\dot{H}+2H^2) = (\epsilon - 2)H^2. \tag{90}$$

We observed in Sec. III B that $\epsilon = 3\dot{\sigma}^2/(\dot{\sigma}^2 + 2V)$, so $0 \leq \epsilon \leq 3$, and hence $m_{4,I}^2/H^2 = \mathcal{O}(1)$ regardless of the couplings and of the motion of the background fields φ^I. Within the single-field attractor (with $\chi \sim \dot{\chi} \sim 0$), many of the other terms in Eq. (89) also become negligible. In particular,

$$\mathcal{G}_{\phi\chi} \sim \mathcal{G}^{\phi\chi} \sim \mathcal{O}(\chi) \sim 0,$$

$$\Gamma^\phi{}_{\phi\chi} \sim \Gamma^\chi{}_{\phi\phi} \sim \Gamma^\chi{}_{\chi\chi} \sim \mathcal{O}(\chi) \sim 0,$$

$$V_{,\chi} \sim V_{,\phi\chi} \sim \mathcal{O}(\chi) \sim 0. \tag{91}$$

Upon using the expressions for $\mathcal{G}_{IJ}$, $\Gamma^I{}_{JK}$, and $\mathcal{R}_{ILMJ}$ in Appendix A, we then find

$$m_{1,\phi}^2 = \mathcal{G}^{\phi\phi}[V_{,\phi\phi} - \Gamma^\phi{}_{\phi\phi}V_{,\phi}] + \mathcal{O}(\chi^2),$$

$$m_{2,\phi}^2 = \mathcal{O}(\chi\dot{\chi}) \sim 0,$$

$$m_{3,\phi}^2 = -\frac{\mathcal{G}_{\phi\phi}}{M_{\rm pl}^2}\left[(3+\epsilon)\dot{\phi}^2 + \frac{2}{H}\dot{\phi}\ddot{\phi}\right] + \mathcal{O}(\chi\dot{\chi}),$$

$$m_{1,\chi}^2 = \mathcal{G}^{\chi\chi}[V_{,\chi\chi} - \Gamma^\phi{}_{\chi\chi}V_{,\phi}] + \mathcal{O}(\chi^2),$$

$$m_{2,\chi}^2 = \frac{1}{2}\mathcal{R}\mathcal{G}_{\phi\phi}\dot{\phi}^2 + \mathcal{O}(\chi\dot{\chi}),$$

$$m_{3,\chi}^2 = \mathcal{O}(\chi\dot{\chi}) \sim 0. \tag{92}$$

The $\mathcal{R}$ in $m_{2,\chi}^2$ is the Ricci curvature scalar of the field-space manifold, an explicit expression for which may be found in Eq. (A6) in Appendix A.

As shown in Fig. 11, there exist three distinct regimes of interest, depending on whether $\xi_I < \mathcal{O}(1)$, $\xi_I \sim \mathcal{O}(1$–$10)$, or $\xi_I \geq \mathcal{O}(100)$. Both $m_{\rm eff,\phi}^2$ and $m_{\rm eff,\chi}^2$ develop increasingly

sharp features with increasing ξ_I, an effect studied in Ref. [56] and further explored in Refs. [1,2]. These sharp features lead to spikes in $\partial_t m_{\rm eff,I}^2$ (and hence in $\mathcal{A}_{(I)}$) for both adiabatic and isocurvature modes for $\xi_I \geq \mathcal{O}(100)$, yielding efficient particle production in that limit. Other effects are notable in Fig. 11. For example, for the adiabatic modes, the term arising from the coupled metric perturbations, $m_{3,\phi}^2$, becomes increasingly important as ξ_I becomes large, periodically driving $m_{\rm eff,\phi}^2 < 0$ and hence yielding brief, tachyonic bursts of particle production, an effect we study in more detail in Ref. [2].

On the other hand, for intermediate values of the nonminimal couplings, $\xi_I \sim \mathcal{O}(10)$, we see that $m_{\rm eff,\chi}^2$ neither becomes sharply peaked nor oscillates to zero. In the intermediate regime, therefore, we expect suppressed amplification of the isocurvature modes. We may understand this suppression analytically. Along the isocurvature direction, $m_{2,\chi}^2 \propto \dot{\phi}^2$ may become comparable in magnitude, but opposite in phase, to $m_{1,\chi}^2 \propto \phi^2$ depending on the magnitude of ξ_I. For $\xi_I < 1$, we may expand

$$m_{1,\chi}^2 = \frac{gM_{\rm pl}^2}{\xi_\phi}\delta^2\left[1 - \delta^2\left(1 + \frac{\lambda_\phi}{g}(2-\epsilon)\right)\right] + \mathcal{O}(\xi_I^2), \tag{93}$$

where δ^2 is defined in Eq. (24) and the eccentricity ε is defined in Eq. (27). In the same limit, we have

$$m_{2,\chi}^2 = \left(\frac{\dot{\phi}^2}{M_{\rm pl}^4}\right)[\xi_\phi + \xi_\chi] + \mathcal{O}(\xi_I^2). \tag{94}$$

For an order-of-magnitude estimate in this limit, we may approximate $\dot{\phi}^2 \sim \omega^2\phi^2$ and use our results from Sec. III C. For $\xi_I \sim 0.1$, we have $\omega = 2\pi/T \rightarrow (2\pi/3.9)\sqrt{\lambda_\phi}M_{\rm pl}$ and hence

$$\frac{m_{2,\chi}^2}{m_{1,\chi}^2} \sim \frac{\lambda_\phi}{g}(\xi_\phi + \xi_\chi) + \mathcal{O}(\xi_I^2). \tag{95}$$

For $\xi_I < 1$, we therefore find a clear separation of scales, $m_{2,\chi}^2 \ll m_{1,\chi}^2$. In that limit, $m_{\rm eff,\chi}^2$ passes near zero as the background field $\phi(t)$ oscillates, as shown in Fig. 11(b). For $\xi_I \sim 10$, however, we find

$$m_{1,\chi}^2 = -\frac{\Lambda_\phi}{\xi_\phi^2}M_{\rm pl}^2\left(\frac{\delta^2}{1+\delta^2}\right) + \mathcal{O}(\xi_I^{-2}), \tag{96}$$

where Λ_ϕ is defined in Eq. (27). For $\xi_I \sim 10$, the parameter $\delta^2 \sim \mathcal{O}(1)$ at the end of inflation. Upon using Eq. (A6), we find

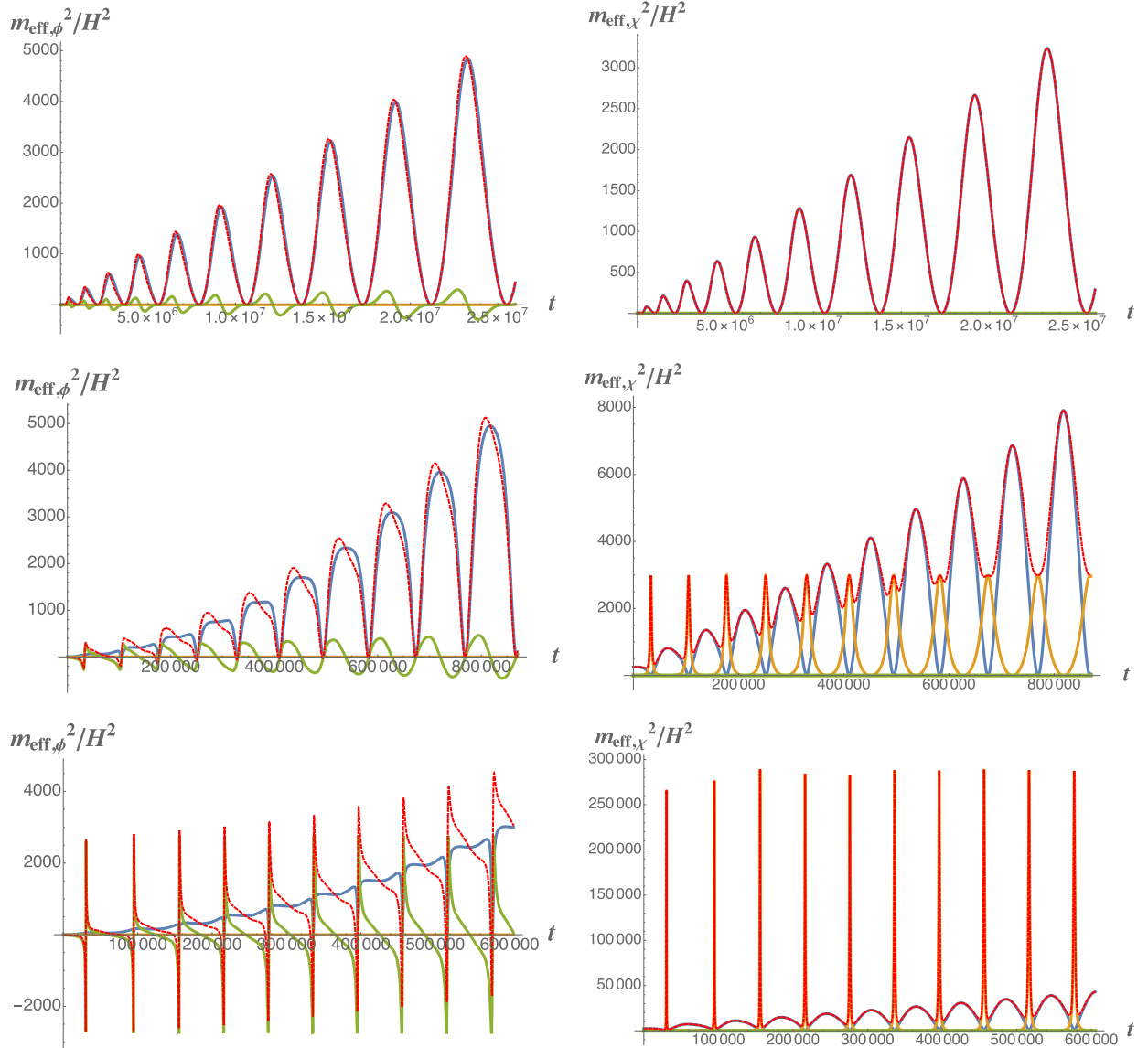$$m_{2,\chi}^2 = \frac{6\xi_\phi\xi_\chi}{M_{\rm pl}^2}\dot{\phi}^2 + \mathcal{O}(\xi_I). \tag{97}$$

FIG. 11. The contributions to $m^2_{\text{eff},\phi}$ (left) and $m^2_{\text{eff},\chi}$ (right) as functions of t; inflation ends and preheating begins at $t = 0$. In each plot, we show the individual contributions to $m^2_{\text{eff},I}$: $m^2_{1,I}$ (blue) arising from the potential; $m^2_{2,I}$ (gold) arising from the curved field-space manifold; $m^2_{3,I}$ (green) arising from the coupled metric perturbations. The contribution $m^2_{4,I}$ is not plotted (since it remains so small), though it is included numerically in our solutions for $m^2_{\text{eff},I}/H^2$ (red dashed). For each plot, we fix $\sqrt{\lambda_\phi}/\xi_\phi = 10^{-4}$, $\xi_\chi/\xi_\phi = 0.8$, $\lambda_\chi/\lambda_\phi = 1.25$, and $g/\lambda_\phi = 2$, and vary ξ_ϕ: $\xi_\phi = 0.1$ (top); $\xi_\phi = 10$ (middle); $\xi_\phi = 100$ (bottom). The quantity $m^2_{\text{eff},I}/H^2$ grows over time because $H(t)$ falls after the end of inflation.

Again making use of our results in Sec. III C to replace $\dot{\phi}^2 \sim \omega^2 \phi^2$, now with $\xi_I \sim 10$, we have $\omega = 2\pi/T \rightarrow (2\pi/14.8)\sqrt{\lambda_\phi}M_{\text{pl}}/\xi_\phi$, which yields

$$\frac{m^2_{2,\chi}}{m^2_{1,\chi}} \sim \frac{\lambda_\phi \xi_\chi}{|\Lambda_\phi|} \sim \mathcal{O}(1). \tag{98}$$

Therefore we do indeed expect $m^2_{1,\chi}$ and $m^2_{2,\chi}$ to remain comparable in magnitude but opposite in phase for $\xi_I \sim \mathcal{O}(10)$. In that case, $m^2_{\text{eff},\chi}$ never passes through zero, as shown in Fig. 11(d). Meanwhile, for $\xi_I \geq \mathcal{O}(100)$, the

oscillations of $\phi(t)$ become sufficiently different from the near-harmonic case that $\dot{\phi}^2 \gg \omega^2 \phi^2$ [1,2,56], and we find that $m^2_{2,\chi} \gg m^2_{1,\chi}$, as shown in Fig. 11(f). The intermediate-ξ_I regime is thus characterized by efficient growth of adiabatic perturbations, with $|\mathcal{A}_{(\phi)}| > 1$, but suppression of isocurvature perturbations, with $|\mathcal{A}_{(\chi)}| < 1$, as shown in Fig. 12.

C. Rotating the field-space coordinates

Now consider what happens when we change the couplings so that the single-field attractor lies along some
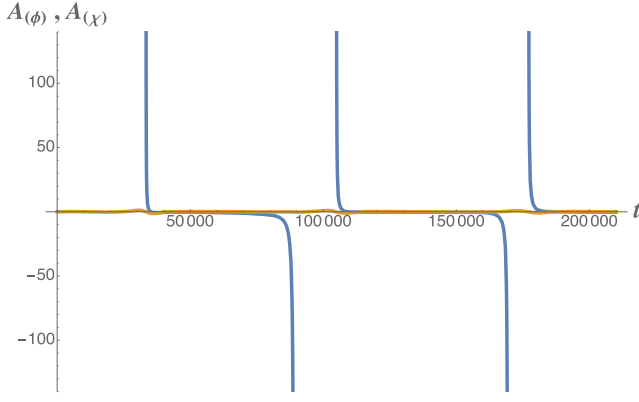
FIG. 12. The adiabatic parameters $\mathcal{A}_{(\phi)}$ (blue) and $\mathcal{A}_{(\chi)}$ (gold) for $k \ll aH$ and $\xi_\phi = 10$, with the ratios of couplings as in Fig. 11. In the intermediate regime, with $\xi_I \sim \mathcal{O}(10)$, adiabatic perturbations are amplified while isocurvature modes are suppressed.
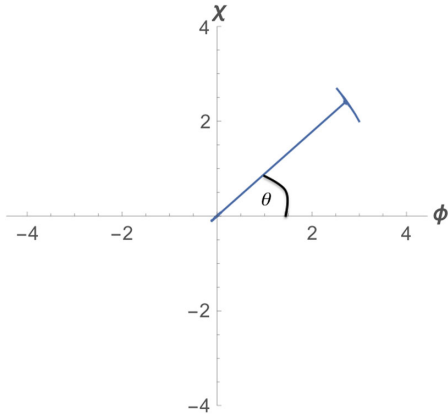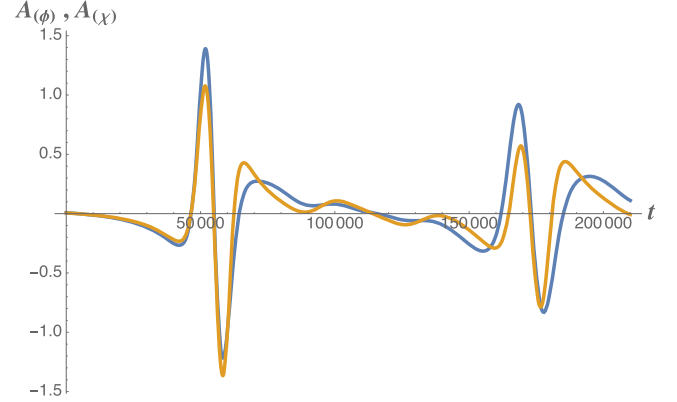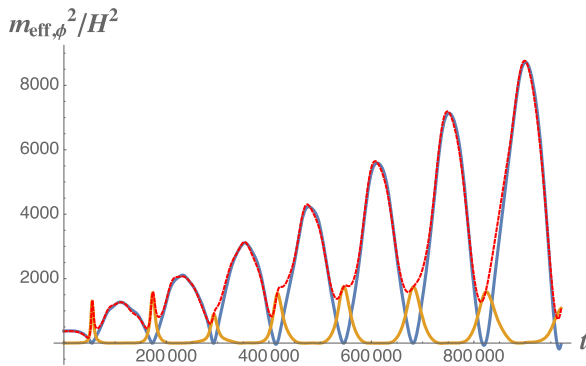

FIG. 15. The adiabatic parameters $\mathcal{A}_{(\phi)}$ and $\mathcal{A}_{(\chi)}$ for the original coordinate bases, with $\xi_\phi = 10$, $g = -1/2$, and the other couplings as in Eq. (99). Because $m^2_{2,I}$ remains comparable in magnitude but opposite in phase to $m^2_{1,I}$, neither $\mathcal{A}_{(\phi)}$ nor $\mathcal{A}_{(\chi)}$ grows much larger than 1.

FIG. 13. For some choices of the coupling constants, the background fields evolve along a single-field trajectory at some angle θ that does not coincide with either the ϕ or χ axes. Shown here is the case for $\xi_\chi/\xi_\phi = 0.8$, $\lambda_\chi/\lambda_\phi = 1.25$, $g/\lambda_\phi = -1/2$, with $\xi_\phi = 10$, $\lambda_\phi = 10^{-6}$. The angle, $\theta = \arctan(\chi/\phi)$, is independent of time during as well as after inflation.

distinct direction in field space. For example, we may select the couplings

$$\frac{\lambda_\chi}{\lambda_\phi} = 1.25, \qquad \frac{g}{\lambda_\phi} = -1/2, \qquad \frac{\xi_\chi}{\xi_\phi} = 0.8. \qquad (99)$$

For minimally coupled models, $g < 0$ leads to an explosive "negative coupling instability" for long-wavelength modes [116,117]. In the presence of nonminimal couplings, however, at least for $|g| \sim \mathcal{O}(\lambda_\phi)$, the effect of the negative coupling is to rotate the orientation of the valley of the potential away from the direction $\chi = 0$. See Fig. 13. With the fields' motion "misaligned" with respect to the original axes of our field-space coordinate system, we find suppression of the resonances along *both* of the original axes, since in this case $m^2_{2,I}$ remains comparable in magnitude (but opposite in phase) with $m^2_{1,I}$ for both $m^2_{\mathrm{eff},\phi}$ and $m^2_{\mathrm{eff},\chi}$. See Fig. 14. Therefore both $\mathcal{A}_{(\phi)}$ and $\mathcal{A}_{(\chi)}$ remain $\mathcal{O}(1)$, as shown in Fig. 15.
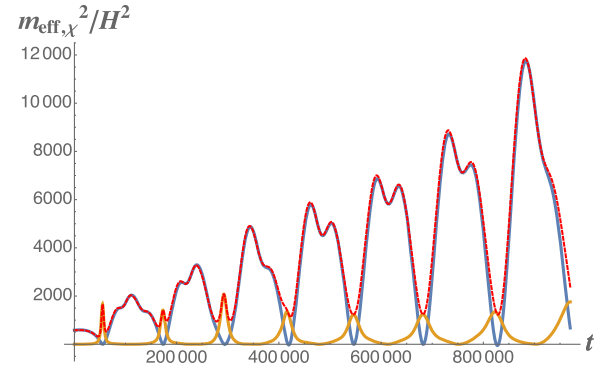

FIG. 14. Left: terms $m^2_{1,\phi}$ (blue) and $m^2_{2,\phi}$ (gold) compared to $m^2_{\mathrm{eff},\phi}$ (red dashed) for $\xi_\phi = 10$, $g = -1/2$, and the other couplings as in Eq. (99). When plotted with respect to the original coordinate bases, $m^2_{\mathrm{eff},\phi}$ no longer oscillates through zero. Right: terms $m^2_{1,\chi}$ (blue) and $m^2_{2,\chi}$ (gold) compared to $m^2_{\mathrm{eff},\chi}$ (red dashed) for $\xi_\phi = 10$, $g = -1/2$, and the other couplings as in Eq. (99).
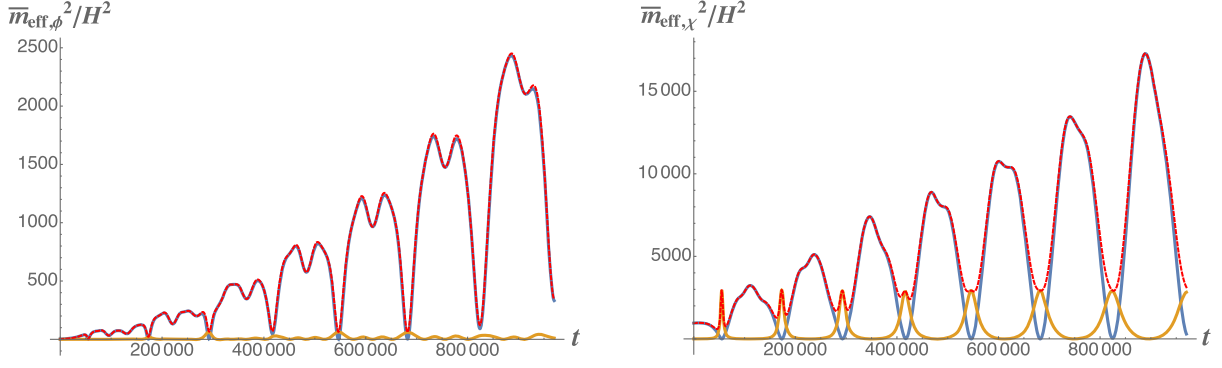
FIG. 16. Left: contributions $\bar{m}_{1,\phi}^2$ (blue) and $\bar{m}_{2,\phi}^2$ (gold) to $\bar{m}_{\text{eff},\phi}^2$ (red dashed), upon making the rotation in field space, for $\xi_\phi = 10$, $g = -1/2$, and the other couplings as in Eq. (99). Unlike in Fig. 14, here we find the contribution from the field-space manifold, $\bar{m}_{2,\phi}^2$, negligible, and hence $\bar{m}_{\text{eff},\phi}^2 \sim \bar{m}_{1,\phi}^2$ oscillates through zero. Right: contributions $\bar{m}_{1,\chi}^2$ (blue) and $\bar{m}_{2,\chi}^2$ (gold) to $\bar{m}_{\text{eff},\chi}^2$ (red dashed), upon making the rotation in field space, for $\xi_\phi = 10$, $g = -1/2$, and the other couplings as in Eq. (99). Just as in the case when the single-field attractor lay along the direction $\chi = 0$, in this case we find $\bar{m}_{1,\chi}^2 \sim \bar{m}_{2,\chi}^2$ but out of phase with each other, so that $\bar{m}_{\text{eff},\chi}^2$ never oscillates through zero.

However, as Fig. 13 makes clear, in this case the fields still evolve within a single-field attractor. We may parametrize the motion by a single angle, $\theta \equiv \arctan(\chi/\phi)$, which, following an initial transient, does not vary over time (even after the end of inflation). That is, when plotted in the original coordinate system, the background fields' motion obeys

$$\phi(t) = r(t)\cos\theta, \qquad \chi(t) = r(t)\sin\theta. \qquad (100)$$

We may then perform a rotation of our coordinates in field space so that the single-field attractor lies along the $\bar{\chi}$ direction, with all motion of the background fields along the $\bar{\phi}$ axis. (In this subsection we denote the rotated coordinate system with an overbar rather than a prime, to avoid confusion with derivatives, $d/d\eta$.) Hence we may write

$$\bar{\phi} = \phi\cos\theta + \chi\sin\theta,$$
$$\bar{\chi} = \chi\cos\theta - \phi\sin\theta. \qquad (101)$$

Components of the tensor $[\omega_k^2]^I{}_J$ transform in the usual way under this coordinate transformation:

$$[\bar{\omega}_k^2]^I{}_J = \left(\frac{\partial\bar{\varphi}^I}{\partial\varphi^K}\right)\left(\frac{\partial\varphi^L}{\partial\bar{\varphi}^J}\right)[\omega_k^2]^K{}_L. \qquad (102)$$

In particular, we find

$$[\bar{\omega}_k^2]^{\phi}{}_{\phi} = \cos^2\theta[\omega_k^2]^{\phi}{}_{\phi} + \sin\theta\cos\theta([\omega_k^2]^{\chi}{}_{\phi} + [\omega_k^2]^{\phi}{}_{\chi})$$
$$+ \sin^2\theta[\omega_k^2]^{\chi}{}_{\chi},$$
$$[\bar{\omega}_k^2]^{\chi}{}_{\chi} = \cos^2\theta[\omega_k^2]^{\chi}{}_{\chi} - \sin\theta\cos\theta([\omega_k^2]^{\phi}{}_{\chi} + [\omega_k^2]^{\chi}{}_{\phi})$$
$$+ \sin^2\theta[\omega_k^2]^{\phi}{}_{\phi}. \qquad (103)$$

When plotted with respect to the rotated coordinate system, we recover the type of behavior we had found in Sec. IV B for

a single-field attractor along the direction $\chi = 0$. Figure 16 shows the dominant contributions to $\bar{m}_{\text{eff},\phi}^2$, revealing that in the rotated coordinate system, the contributions from the field-space manifold become negligible, just as they do for $m_{\text{eff},\phi}^2$ when the single-field attractor lies along the $\chi = 0$ direction (as in Fig. 11). On the other hand, in the rotated coordinate basis, $\bar{m}_{2,\chi}^2$ remains comparable in magnitude to $\bar{m}_{1,\chi}^2$ but with opposite phase, so that $\bar{m}_{\text{eff},\chi}^2$ never oscillates through zero (again like the behavior in Fig. 11). Moreover, if we compute

$$\bar{\mathcal{A}}_{(I)} = \frac{\partial_t \bar{m}_{\text{eff},I}^2}{2(\bar{m}_{\text{eff},I}^2)^{3/2}} + \frac{H}{\bar{m}_{\text{eff},I}}, \qquad (104)$$

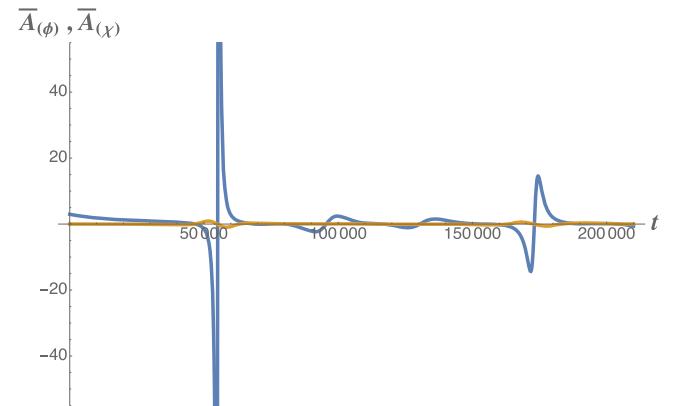FIG. 17. The adiabatic parameters $\bar{\mathcal{A}}_{(\phi)}$ (blue) and $\bar{\mathcal{A}}_{(\chi)}$ (gold) with $\xi_\phi = 10$, $g = -1/2$, and the other couplings as in Eq. (99), upon performing the rotation in field space. Here we recover behavior akin to the original example, when the single-field attractor lies along the direction $\chi = 0$: fluctuations along the adiabatic direction become strongly amplified, but those in the isocurvature direction do not.

we find behavior akin to the original analysis for the $\chi = 0$ attractor, as shown in Fig. 17. Thus we surmise that within *any* single-field attractor, in the intermediate regime with $\xi_I \sim \mathcal{O}(10)$, we find suppression of the resonances for the isocurvature direction and amplification of the fluctuations along the adiabatic direction. This general result holds even though the models we consider do not obey an $O(N)$ symmetry.

V. CONCLUSIONS

Realistic models of high-energy physics typically include multiple scalar fields, each with its own non-minimal coupling. In this paper we have demonstrated that preheating after inflation in such models introduces unique features that are distinct from other well-studied models of preheating.

In particular, nonminimally coupled fields yield a conformally stretched effective potential in the Einstein frame. In previous work we had highlighted a generic feature that arises from such conformal stretching, namely, the existence of strong single-field attractor behavior across a wide range of couplings and initial conditions [44–47]. Here we have found two main effects related to the conformal stretching and attractor behavior: the effectively single-field evolution of the background fields $\varphi^I(t)$ persists during the oscillatory phase—thereby avoiding the "dephasing" that is typical of preheating with minimally coupled scalar fields—and the conformal stretching of the potential alters the time evolution of $\varphi^I(t)$ as the background field(s) oscillate around the global minimum of the potential.

The persistence of the single-field attractor during the preheating phase leads to efficient transfer of energy from the background fields to coupled fluctuations. The balance of the transfer to fluctuations in the adiabatic versus isocurvature directions depends on the nonminimal coupling constants. We identify here, and study further in Refs. [1,2], three distinct regimes, depending on whether $\xi_I < \mathcal{O}(1)$, $\xi_I \sim \mathcal{O}(1-10)$, or $\xi_I \geq \mathcal{O}(100)$. The growth of long-wavelength isocurvature modes is suppressed for intermediate couplings, $\xi_I \sim \mathcal{O}(10)$—a new effect arising entirely from the nontrivial field-space manifold, which has no analog in models with minimally coupled fields. In the large-ξ_I regime, however, appropriate to such models as Higgs inflation [48], the amplification of isocurvature modes becomes very efficient [1,2,56]. (Naturally, the efficient amplification of isocurvature perturbations after the end of inflation is quite distinct from the amplification of isocurvature perturbations during inflation, which is generically suppressed in these models [47]. Modes amplified during inflation would have length scales today of tens to thousands of Mpc, due to their exponential stretching during inflation; modes amplified after the end of inflation would have exponentially shorter length scales, and would not affect observables such as β_{iso}.)

The efficiency of the reheating stage can have observational consequences, both for the CMB and for the particle content of the Universe. The values of the CMB observables n_s and r may be related to the time N_*, where N_* is the number of efolds before the end of inflation when perturbations on CMB-relevant length scales crossed outside the Hubble radius. For models in the family we consider here, these relations are given by $n_s \simeq 1\text{–}2/N_* - 3/N_*^2$ and $r \simeq 12/N_*^2$ (see, e.g., Ref. [46]). Depending on how quickly the Universe transitions to a radiation-dominated phase after the end of inflation, the observationally relevant N_* may vary by as much as 10 efolds (see, e.g., Ref. [24]), shifting the predictions for r by as much as 30% and for $n_s - 1$ by as much as 10%. Furthermore, different reheating scenarios can yield different reheat temperatures, which can have other implications, such as washing out lepton or baryon asymmetries that might have been generated at the end of inflation. Such possibilities make it critical to gain an understanding of the reheating process following inflation.

In Refs. [1,2] we exploit the covariant formalism developed here to more thoroughly explore the resonance structure in this family of models as functions of wave number, k, as well as coupling constants, ξ_I, λ_I, and g. Other effects also deserve further attention. In particular, the conformal stretching of the potential in the Einstein frame could produce metastable oscillons after inflation. The formation of such long-lived, topologically metastable objects could become important after the earliest stages of preheating, impacting the rate at which the system ultimately reaches thermal equilibrium. These and related nonlinear effects could therefore affect the final reheat temperature and the expansion history of the Universe after inflation [118–122]. These possibilities remain the subject of further research.

APPENDIX A: FIELD-SPACE METRIC AND RELATED QUANTITIES

Given $f(\phi^I)$ in Eq. (19) for a two-field model, the field-space metric in the Einstein frame, Eq. (5), takes the form

$$
\mathcal{G}_{\phi\phi} = \left(\frac{M_{\mathrm{pl}}^2}{2f}\right)\left[1 + \frac{3\xi_\phi^2\phi^2}{f}\right],
$$
$$
\mathcal{G}_{\phi\chi} = \mathcal{G}_{\chi\phi} = \left(\frac{M_{\mathrm{pl}}^2}{2f}\right)\left[\frac{3\xi_\phi\xi_\chi\phi\chi}{f}\right],
$$
$$
\mathcal{G}_{\chi\chi} = \left(\frac{M_{\mathrm{pl}}^2}{2f}\right)\left[1 + \frac{3\xi_\chi^2\chi^2}{f}\right]. \tag{A1}
$$

The components of the inverse metric are

$$
\mathcal{G}^{\phi\phi} = \left(\frac{2f}{M_{\mathrm{pl}}^2}\right)\left[\frac{2f + 6\xi_\chi^2\chi^2}{C}\right],
$$
$$
\mathcal{G}^{\phi\chi} = \mathcal{G}^{\chi\phi} = -\left(\frac{2f}{M_{\mathrm{pl}}^2}\right)\left[\frac{6\xi_\phi\xi_\chi\phi\chi}{C}\right],
$$
$$
\mathcal{G}^{\chi\chi} = \left(\frac{2f}{M_{\mathrm{pl}}^2}\right)\left[\frac{2f + 6\xi_\phi^2\phi^2}{C}\right], \tag{A2}
$$

where $C(\phi^I)$ is defined as

$$
\begin{aligned}
C(\phi,\chi) &\equiv M_{\mathrm{pl}}^2 + \xi_\phi(1 + 6\xi_\phi)\phi^2 + \xi_\chi(1 + 6\xi_\chi)\chi^2 \\
&= 2f + 6\xi_\phi^2\phi^2 + 6\xi_\chi^2\chi^2. \tag{A3}
\end{aligned}
$$

The Christoffel symbols for our field space take the form

$$
\Gamma^\phi_{\phi\phi} = \frac{\xi_\phi(1 + 6\xi_\phi)\phi}{C} - \frac{\xi_\phi\phi}{f},
$$
$$
\Gamma^\phi_{\chi\phi} = \Gamma^\phi_{\phi\chi} = -\frac{\xi_\chi\chi}{2f},
$$
$$
\Gamma^\phi_{\chi\chi} = \frac{\xi_\phi(1 + 6\xi_\chi)\phi}{C},
$$
$$
\Gamma^\chi_{\phi\phi} = \frac{\xi_\chi(1 + 6\xi_\phi)\chi}{C},
$$
$$
\Gamma^\chi_{\phi\chi} = \Gamma^\chi_{\chi\phi} = -\frac{\xi_\phi\phi}{2f},
$$
$$
\Gamma^\chi_{\chi\chi} = \frac{\xi_\chi(1 + 6\xi_\chi)\chi}{C} - \frac{\xi_\chi\chi}{f}. \tag{A4}
$$

For two-dimensional manifolds we may always write the Riemann tensor in the form

$$
\mathcal{R}_{ABCD} = \frac{1}{2}\mathcal{R}(\phi^I)[\mathcal{G}_{AC}\mathcal{G}_{BD} - \mathcal{G}_{AD}\mathcal{G}_{BC}], \tag{A5}
$$

where $\mathcal{R}(\phi^I)$ is the Ricci scalar. Given the field-space metric of Eq. (A1), we find

$$
\mathcal{R}(\phi^I) = \frac{1}{3M_{\mathrm{pl}}^2 C^2}[(1 + 6\xi_\phi)(1 + 6\xi_\chi)(4f^2) - C^2]. \tag{A6}
$$

For the two-field model, we may also solve explicitly for the vielbeins, e_b^I, of Eq. (64). Defining

$$
A \equiv C - 6\xi_\phi^2\phi^2,
$$
$$
B \equiv C - 6\xi_\chi^2\chi^2,
$$
$$
E \equiv C - 3\xi_\phi^2\phi^2 - 3\xi_\chi^2\chi^2,
$$
$$
F \equiv \frac{\sqrt{2fC}\sqrt{E - \sqrt{2fC}}}{3\sqrt{2}M_{\mathrm{pl}}(\xi_\chi^2\chi^2 + \xi_\phi^2\phi^2)C}, \tag{A7}
$$

then we may satisfy Eq. (64) with

$$
e_1^\phi = F(A + \sqrt{2fC}),
$$
$$
e_1^\chi = -6F\xi_\phi\xi_\phi\phi\chi,
$$
$$
e_2^\phi = e_1^\chi,
$$
$$
e_2^\chi = F(B + \sqrt{2fC}). \tag{A8}
$$

We note that within the single-field attractor along the direction $\chi = 0$, $e_2^\phi \sim e_1^\chi \sim 0$, $e_1^\phi e_1^\phi \to \mathcal{G}^{\phi\phi} + \mathcal{O}(\chi^2)$, and $e_2^\chi e_2^\chi \to \mathcal{G}^{\chi\chi} + \mathcal{O}(\chi^2)$.

APPENDIX B: PERIOD OF SINGLE-FIELD BACKGROUND OSCILLATIONS

Starting from Eq. (50) and inserting the values of $\mathcal{G}_{\phi\phi}$ and $V(\phi)$ the period becomes

$$
T = 4\sqrt{2\xi_\phi}\int_0^\alpha du \frac{\sqrt{1 + 6\xi_\phi u^2}}{(1 + u^2)}\frac{1}{\sqrt{\frac{\alpha^4}{(1+\alpha^2)^2} - \frac{u^4}{(1+u^2)^2}}} \tag{B1}
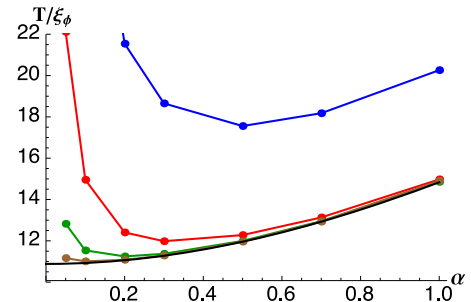$$

FIG. 18. Period of oscillation, T, rescaled by the nonminimal coupling, in units of $(\sqrt{\lambda_\phi}M_{\mathrm{pl}})^{-1}$, as a function of $\alpha = \sqrt{\xi_\phi}\phi_0/M_{\mathrm{pl}}$ for $\xi = 10, 10^2, 10^3, 10^4$ (from top to bottom). The solid black line shows the approximate analytic result of Eq. (51), which is derived under the assumption that $6\xi_\phi\alpha^2 \gg 1$.

where we made a change of variables $u = \sqrt{\xi_\phi}\phi$, and parametrized the maximum field amplitude as $\phi_{\max} = \alpha M_{pl}/\sqrt{\xi_\phi}$. By assuming a maximum field amplitude such that $1 < 6\xi_\phi\alpha^2$ and approximating $1 + 6\xi_\phi u^2 \approx 6\xi_\phi u^2$, the integral can be performed analytically and the resulting Eq. (51) shows the linear scaling of the period with ξ_ϕ. The limit of this

approximation is shown in Fig. 18, where it can be seen that the agreement between Eq. (51) and the exact result is excellent in the large-ξ_I limit for α not very small. The region of validity in terms of α increases for larger values of ξ_ϕ, as expected from the condition $\alpha > 1/\sqrt{6\xi_\phi}$ used in the derivation of Eq. (51). Figure 18 shows the period of oscillation for different values of ξ_I and α.

[1] M. P. DeCross, D. I. Kaiser, A. Prabhu, C. Prescod-Weinstein, and E. I. Sfakianakis, following paper, Preheating in multifield inflation with nonminimal couplings. II. Resonance structure, Phys. Rev. D **97**, 023527 (2018).

[2] M. P. DeCross, D. I. Kaiser, A. Prabhu, C. Prescod-Weinstein, and E. I. Sfakianakis, Preheating in multifield inflation with nonminimal couplings. III. Dynamical spacetime results, Phys. Rev. D **97**, 023528 (2018).

[3] A. H. Guth and D. I. Kaiser, Inflationary cosmology: Exploring the universe from the smallest to the largest scales, Science **307**, 884 (2005).

[4] B. A. Bassett, S. Tsujikawa, and D. Wands, Inflation dynamics and reheating, Rev. Mod. Phys. **78**, 537 (2006).

[5] D. H. Lyth and A. R. Liddle, *The Primordial Density Perturbation: Cosmology, Inflation, and the Origin of Structure* (Cambridge University Press, New York, 2009).

[6] D. Baumann, TASI Lectures on inflation, arXiv:0907.5424.

[7] J. Martin, C. Ringeval, and V. Vennin, Encyclopedia inflationaris, Phys. Dark Universe **5–6**, 75 (2014).

[8] A. H. Guth, D. I. Kaiser, and Y. Nomura, Inflationary paradigm after Planck 2013, Phys. Lett. B **733**, 112 (2014).

[9] A. D. Linde, Inflationary cosmology after Planck 2013, arXiv:1402.0526.

[10] J. Martin, The observational status of cosmic inflation after Planck, Astrophys. Space Sci. **45**, 41 (2016).

[11] G. Steigman, Primordial nucleosynthesis in the precision cosmology era, Annu. Rev. Nucl. Part. Sci. **57**, 463 (2007).

[12] B. D. Fields, P. Molaro, and S. Sarkar, Big-bang nucleosynthesis, Chin. Phys. C **38**, 339 (2014).

[13] R. H. Cyburt, B. D. Fields, K. A. Olive, and T.-H. Yeh, Big bang nucleosynthesis: 2015, Rev. Mod. Phys. **88**, 015004 (2016).

[14] P. Adshead, R. Easther, J. Pritchard, and A. Loeb, Inflation and the scale dependent spectral index: Prospects and strategies, J. Cosmol. Astropart. Phys. 02 (2011) 021.

[15] L. Dai, M. Kamionkowski, and J. Wang, Reheating Constraints to Inflationary Models, Phys. Rev. Lett. **113**, 041302 (2014).

[16] P. Creminelli, D. L. Nacir, M. Simonovi, G. Trevisan, and M. Zaldarriaga, φ^2 inflation at its endpoint, Phys. Rev. D **90**, 083513 (2014).

[17] J. Martin, C. Ringeval, and V. Vennin, Observing the Inflationary Reheating, Phys. Rev. Lett. **114**, 081303 (2015).

[18] J.-O. Gong, G. Leung, and S. Pi, Probing reheating with primordial spectrum, J. Cosmol. Astropart. Phys. 05 (2015) 027.

[19] R.-G. Cai, Z.-K. Guo, and S.-J. Wang, Reheating phase diagram for single-field slow-roll inflationary models, Phys. Rev. D **92**, 063506 (2015).

[20] J. L. Cook, E. Dimastrogiovanni, D. A. Easson, and L. M. Krauss, Reheating predictions in single field inflation, J. Cosmol. Astropart. Phys. 04 (2015) 047.

[21] V. Domcke and J. Heisig, Constraints on the reheating temperature from sizable tensor modes, Phys. Rev. D **92**, 103515 (2015).

[22] R. Allahverdi, R. Brandenberger, F.-Y. Cyr-Racine, and A. Mazumdar, Reheating in inflationary cosmology: Theory and applications, Annu. Rev. Nucl. Part. Sci. **60**, 27 (2010).

[23] A. V. Frolov, Non-linear dynamics and primordial curvature perturbations from preheating, Classical Quantum Gravity **27**, 124006 (2010).

[24] M. A. Amin, M. P. Hertzberg, D. I. Kaiser, and J. Karouby, Nonperturbative dynamics of reheating after inflation: A review, Int. J. Mod. Phys. D **24**, 1530003 (2015).

[25] M. A. Amin and D. Baumann, From wires to cosmology, J. Cosmol. Astropart. Phys. 02 (2016) 045.

[26] M. P. Hertzberg and J. Karouby, Baryogenesis from the inflaton field, Phys. Lett. B **737**, 34 (2014); Generating the observed baryon asymmetry from the inflaton field, Phys. Rev. D **89**, 063523 (2014).

[27] P. Adshead and E. I. Sfakianakis, Leptogenesis from Left-Handed Neutrino Production during Axion Inflation, Phys. Rev. Lett. **116**, 091301 (2016).

[28] P. Adshead and E. I. Sfakianakis, Fermion production during and after axion inflation, J. Cosmol. Astropart. Phys. 11 (2015) 021.

[29] K. D. Lozanov and M. A. Amin, End of inflation, oscillons, and matter-antimatter asymmetry, Phys. Rev. D **90**, 083528 (2014).

[30] D. H. Lyth and A. Riotto, Particle physics models of inflation and the cosmological density perturbation, Phys. Rep. **314**, 1 (1999).

[31] D. Wands, Multiple field inflation, Lect. Notes Phys. **738**, 275 (2008).

[32] A. Mazumdar and J. Rocher, Particle physics models of inflation and curvaton scenarios, Phys. Rep. **497**, 85 (2011).

[33] V. Vennin, K. Koyama, and D. Wands, Encylopedia Curvatonis, J. Cosmol. Astropart. Phys. 11 (2015) 008.

[34] J.-O. Gong, Multi-field inflation and cosmological perturbations, Int. J. Mod. Phys. D **26,** 1740003 (2017).

[35] C. G. Callan, Jr., S. R. Coleman, and R. Jackiw, A new improved energy-momentum tensor, Ann. Phys. (N.Y.) **59,** 42 (1970).

[36] T. S. Bunch, P. Panangaden, and L. Parker, On renormalization of $\lambda \phi^4$ field theory in curved space-time, I, J. Phys. A **13,** 901 (1980); T. S. Bunch and P. Panangaden, On renormalization of $\lambda \phi^4$ field theory in curved space-time. II., J. Phys. A **13,** 919 (1980).

[37] N. D. Birrell and P. C. W. Davies, *Quantum Fields in Curved Space* (Cambridge University Press, New York, 1982).

[38] I. L. Buchbinder, S. D. Odintsov, and I. L. Shapiro, *Effective Action in Quantum Gravity* (Taylor and Francis, New York, 1992).

[39] L. E. Parker and D. J. Toms, *Quantum Field Theory in Curved Spacetime* (Cambridge University Press, New York, 2009).

[40] S. D. Odintsov, Renormalization group, effective action, and grand unification theories in curved spacetime, Fortschr. Phys. **39,** 621 (1991).

[41] T. Markkanen and A. Tranberg, A simple method for one-loop renormalization in curved spacetime, J. Cosmol. Astropart. Phys. 08 (2013) 045.

[42] As is well known, models with gravitational actions of the general form $f(R)$, where R is the spacetime Ricci scalar, may be rewritten in the form of an Einstein-Hilbert action plus a scalar field with nonminimal coupling, $\xi \phi^2 R$ [43]. Hence the formalism we develop here may help illuminate processes in still broader classes of models, though such explorations remain beyond the scope of this paper.

[43] T. P. Sotiriou and V. Faraoni, $f(R)$ theories of gravity, Rev. Mod. Phys. **82,** 451 (2010).

[44] D. I. Kaiser, E. A. Mazenc, and E. I. Sfakianakis, Primordial bispectrum from multifield inflation with nonminimal couplings, Phys. Rev. D **87,** 064004 (2013).

[45] R. N. Greenwood, D. I. Kaiser, and E. I. Sfakianakis, Multifield dynamics of Higgs inflation, Phys. Rev. D **87,** 064021 (2013).

[46] D. I. Kaiser and E. I. Sfakianakis, Multifield Inflation after Planck: The Case for Nonminimal Couplings, Phys. Rev. Lett. **112,** 011302 (2014).

[47] K. Schutz, E. I. Sfakianakis, and D. I. Kaiser, Multifield inflation after Planck: Isocurvature modes from nonminimal couplings, Phys. Rev. D **89,** 064044 (2014).

[48] F. L. Bezrukov and M. E. Shaposhnikov, The Standard Model Higgs boson as the inflaton, Phys. Lett. B **659,** 703 (2008).

[49] R. Kallosh and A. Linde, Non-minimal inflationary attractors, J. Cosmol. Astropart. Phys. 10 (2013) 033; Multi-field conformal cosmological attractors, J. Cosmol. Astropart. Phys. 12 (2013) 006; R. Kallosh, A. Linde, and D. Roest, Universal Attractor for Inflation at Strong Coupling, Phys. Rev. Lett. **112,** 011303 (2014); Superconformal inflationary α-attractors, J. High Energy Phys. 11 (2013) 198; M. Galante, R. Kallosh, A. Linde, and D. Roest, Unity of Cosmological Attractors, Phys. Rev. Lett. **114,** 141302 (2015); R. Kallosh and A. Linde, Planck, LHC, and α-attractors, Phys. Rev. D **91,** 083528 (2015); J. J. M. Carrasco, R. Kallosh, and A. Linde, Cosmological attractors and initial conditions for inflation, Phys. Rev. D **92,** 063519 (2015).

[50] B. A. Bassett and S. Liberati, Geometric reheating after inflation, Phys. Rev. D **58,** 021302 (1998).

[51] S. Tsujikawa, K. Maeda, and T. Torii, Resonant particle production with nonminimally coupled scalar fields in preheating after inflation, Phys. Rev. D **60,** 063515 (1999); Preheating with non-minimally coupled scalar fields in higher-curvature inflation models, Phys. Rev. D **60,** 123505 (1999); Preheating of the nonminimally coupled inflaton field, Phys. Rev. D **61,** 103501 (2000).

[52] S. Tsujikawa and B. A. Bassett, A new twist to preheating, Phys. Rev. D **62,** 043510 (2000); When can preheating affect the CMB?, Phys. Lett. B **536,** 9 (2002).

[53] Y. Watanabe and J. White, Multifield formulation of gravitational particle production after inflation, Phys. Rev. D **92,** 023504 (2015).

[54] K. Kannike, G. Hütsi, L. Pizza, A. Racioppi, M. Raidal, A. Salvio, and A. Strumia, Dynamically induced Planck scale and inflation, J. High Energy Phys. 05 (2015) 065; K. Kannike, A. Racioppi, and M. Raidal, Linear inflation from quartic potential, J. High Energy Phys. 01 (2016) 035.

[55] C. van de Bruck, P. Dunsby, and L. E. Paduraru, Reheating and preheating in the simplest extension of Starobinsky inflation, Int. J. Mod. Phys. D **26,** 1750152 (2017).

[56] Y. Ema, R. Jinno, K. Mukaida, and K. Nakayama, Violent preheating in inflation with nonminimal coupling, J. Cosmol. Astropart. Phys. 02 (2017) 045.

[57] F. Bezrukov, D. Gorbunov, and M. Shaposhnikov, On initial conditions for the hot big bang, J. Cosmol. Astropart. Phys. 06 (2009) 029.

[58] J. García-Bellido, D. G. Figueroa, and J. Rubio, Preheating in the Standard Model with the Higgs-inflaton coupled to gravity, Phys. Rev. D **79,** 063531 (2009).

[59] J.-F. Dufaux, D. G. Figueroa, and J. García-Bellido, Gravitational waves from Abelian gauge fields and cosmic strings at preheating, Phys. Rev. D **82,** 083518 (2010).

[60] J. García-Bellido, J. Rubio, and M. Shaposhnikov, Higgs-dilaton cosmology: Are there extra relativistic species?, Phys. Lett. B **718,** 507 (2012).

[61] J. Lachapelle and R. H. Brandenberger, Preheating with non-standard kinetic term, J. Cosmol. Astropart. Phys. 04 (2009) 020.

[62] J. Karouby, B. Underwood, and A. C. Vincent, Preheating with the brakes on: The effects of a speed limit, Phys. Rev. D **84,** 043528 (2011).

[63] H. L. Child, J. T. Giblin, Jr., R. Ribeiro, and D. Seery, Preheating with Nonminimal Kinetic Terms, Phys. Rev. Lett. **111,** 051301 (2013).

[64] J. Zhang, Y. Cai, and Y.-S. Piao, Preheating in a DBI inflation model, arXiv:1307.6529.

[65] A. Ashoorioon, H. Firouzjahi, and M. M. Sheikh-Jabbari, M-flation: Inflation from matrix valued scalar fields, J. Cosmol. Astropart. Phys. 06 (2009) 018; A. Ashoorioon, B. Fung, R. B. Mann, M. Oltean, and M. M. Sheikh-Jabbari,

Gravitational waves from preheating in M-flation, J. Cosmol. Astropart. Phys. 03 (2014) 020.

[66] N. Barnaby, J. Braden, and L. Kofman, Reheating the universe after multi-field inflation, J. Cosmol. Astropart. Phys. 07 (2010) 016.

[67] D. Battefeld and S. Kawai, Preheating after N-flation, Phys. Rev. D **77,** 123507 (2008); D. Battefeld, Preheating after multifield inflation, Nucl. Phys. B, Proc. Suppl. **192–193,** 126 (2009); D. Battefeld, T. Battefeld, and J. T. Giblin, Jr., On the suppression of parametric resonance and the viability of tachyonic preheating after multifield inflation, Phys. Rev. D **79,** 123510 (2009); T. Battefeld, A. Eggemeier, and J. T. Giblin, Jr., Enhanced preheating after multifield inflation: On the importance of being special, J. Cosmol. Astropart. Phys. 11 (2012) 062.

[68] J. M. Bardeen, Gauge invariant cosmological perturbations, Phys. Rev. D **22,** 1882 (1980).

[69] V. F. Mukhanov, Quantum theory of gauge invariant cosmological perturbations, Sov. Phys. JETP **67,** 1297 (1988).

[70] H. Kodama and M. Sasaki, Cosmological perturbation theory, Prog. Theor. Phys. Suppl. **78,** 1 (1984).

[71] V. F. Mukhanov, H. A. Feldman, and R. H. Brandenberger, Theory of cosmological perturbations, Phys. Rep. **215,** 203 (1992).

[72] K. A. Malik and D. Wands, Cosmological perturbations, Phys. Rep. **475,** 1 (2009).

[73] M. Sasaki and E. D. Stewart, A general analytic formula for the spectral index of the density perturbations produced during inflation, Prog. Theor. Phys. **95,** 71 (1996).

[74] C. Gordon, D. Wands, B. A. Bassett, and R. Maartens, Adiabatic and entropy perturbations from inflation, Phys. Rev. D **63,** 023506 (2000).

[75] S. Groot Nibbelink and B. J. W. van Tent, Density perturbations arising from multiple field slow-roll inflation, arXiv:hep-ph/0011325; Scalar perturbations during multiple-field slow-roll inflation, Classical Quantum Gravity **19,** 613 (2002).

[76] D. Wands, N. Bartolo, S. Matarrese, and A. Riotto, An observational test of two-field inflation, Phys. Rev. D **66,** 043520 (2002).

[77] D. Seery and J. E. Lidsey, Primordial non-Gaussianities from multiple-field inflation, J. Cosmol. Astropart. Phys. 09 (2005) 011.

[78] H.-C. Lee, M. Sasaki, E. D. Stewart, T. Tanaka, and S. Yokoyama, A new delta *N* formalism for multi-component inflation, J. Cosmol. Astropart. Phys. 10 (2005) 004.

[79] S. Yokoyama, T. Suyama, and T. Tanaka, Primordial non-Gaussianity in multi-scalar slow-roll inflation, J. Cosmol. Astropart. Phys. 07 (2007) 013; Primordial non-Gaussianity in multiscalar inflation, Phys. Rev. D **77,** 083511 (2008).

[80] D. Langlois and S. Renaux-Petel, Perturbations in generalized multi-field inflation, J. Cosmol. Astropart. Phys. 04 (2008) 017.

[81] C. M. Peterson and M. Tegmark, Testing two-field inflation, Phys. Rev. D **83,** 023522 (2011); Non-Gaussianity in two-field inflation, Phys. Rev. D **84,** 023520 (2011); Testing multifield inflation: A geometric approach, Phys. Rev. D **87,** 103507 (2013).

[82] J.-O. Gong and T. Tanaka, A covariant approach to general field space metric in multifield inflation, J. Cosmol. Astropart. Phys. 03 (2011) 015.

[83] J. Elliston, D. Seery, and R. Tavakol, The inflationary bispectrum with curved field-space, J. Cosmol. Astropart. Phys. 11 (2012) 060.

[84] D. I. Kaiser, Conformal transformations with multiple scalar fields, Phys. Rev. D **81,** 084044 (2010).

[85] H. Abedi and A. M. Abbassi, Gravitational constant in multiple field gravity, J. Cosmol. Astropart. Phys. 05 (2015) 026.

[86] S. Renaux-Petel and K. Turzynski, On reaching the adiabatic limit in multi-field inflation, J. Cosmol. Astropart. Phys. 06 (2015) 010.

[87] I. G. Moss, Vacuum stability and the scaling behaviour of the Higgs-curvature coupling, arXiv:1509.03554.

[88] T. Futamase and K. Maeda, Chaotic inflationary scenario of the universe with a nonminimally coupled "inflaton" field, Phys. Rev. D **39,** 399 (1989).

[89] D. S. Salopek, J. R. Bond, and J. M. Bardeen, Designing density fluctuation spectra in inflation, Phys. Rev. D **40,** 1753 (1989).

[90] R. Fakir, S. Habib, and W. G. Unruh, Cosmological density perturbations with modified gravity, Astrophys. J. **394,** 396 (1992); R. Fakir and W. G. Unruh, Improvement on cosmological chaotic inflation through nonminimal coupling, Phys. Rev. D **41,** 1783 (1990).

[91] N. Makino and M. Sasaki, The density perturbation in the chaotic inflation with nonminimal coupling, Prog. Theor. Phys. **86,** 103 (1991).

[92] D. I. Kaiser, Primordial spectral indices from generalized Einstein theories, Phys. Rev. D **52,** 4295 (1995).

[93] P. A. R. Ade *et al.* (BICEP2/Keck and Planck Collaborations), Joint Analysis of BICEP2/Keck Array and Planck Data, Phys. Rev. Lett. **114,** 101301 (2015); P. A. R. Ade *et al.* (Planck Collaboration), Planck 2015 results, XIII: Cosmological parameters, Astron. Astrophys. **594,** A13 (2016).

[94] F. Bezrukov and D. Gorbunov, Light inflation after LHC8 and WMAP9 results, J. High Energy Phys. 07 (2013) 140.

[95] A. O. Barvinsky, A. Yu. Kamenschik, C. Kieffer, A. A. Starobinsky, and C. F. Steinwachs, Asymptotic freedom in inflationary cosmology with a nonminimally coupled Higgs field, J. Cosmol. Astropart. Phys. 12 (2009) 003; Higgs boson, renormalization group, and naturalness in cosmology, Eur. Phys. J. C **72,** 2219 (2012).

[96] F. Bezrukov, M. Yu. Kalmykov, B. A. Kniehl, and M. E. Shaposhnikov, Higgs boson mass and new physics, J. High Energy Phys. 10 (2012) 140.

[97] K. Allison, Higgs ξ-inflation for the 125–126 GeV Higgs: A two-loop analysis, J. High Energy Phys. 02 (2014) 040.

[98] F. C. Adams, K. Freese, and A. H. Guth, Constraints on the scalar-field potential in inflationary models, Phys. Rev. D **43,** 965 (1991).

[99] D. I. Kaiser, Constraints in the context of induced gravity inflation, Phys. Rev. D **49,** 6347 (1994).

[100] A. H. Guth and E. I. Sfakianakis, Density perturbations in hybrid inflation using a free field theory time-delay approach, arXiv:1210.8128; I. F. Halpern, M. P. Hertzberg, M. A. Joss, and E. I. Sfakianakis, A density spike on

astrophysical scales from an N-field waterfall transition, Phys. Lett. B **748**, 132 (2015).

[101] X. Chen and C. Ringeval, Searching for standard clocks in the primordial universe, J. Cosmol. Astropart. Phys. 08 (2012) 014; X. Chen and M. H. Namjoo, Standard clock in primordial density perturbations and cosmic microwave background, Phys. Lett. B **739**, 285 (2014); X. Chen, M. H. Namjoo, and Y. Wang, Models of the primordial standard clock, J. Cosmol. Astropart. Phys. 02 (2015) 027; Quantum primordial standard clocks, J. Cosmol. Astropart. Phys. 02 (2016) 013.

[102] M. S. Turner, Coherent scalar field oscillations in an expanding universe, Phys. Rev. D **28**, 1243 (1983).

[103] E. Gourgoulhon and S. Bonazzola, A formulation of the virial theorem in general relativity, Classical Quantum Gravity **11**, 443 (1994).

[104] D. I. Kaiser, Post-inflation reheating in an expanding universe, Phys. Rev. D **53**, 1776 (1996).

[105] D. Boyanovsky, H. J. de Vega, R. Holman, and J. Salgado, Analytic and numerical study of preheating dynamics, Phys. Rev. D **54**, 7570 (1996).

[106] D. I. Kaiser, Preheating in an expanding universe: Analytic results for the massless case, Phys. Rev. D **56**, 706 (1997); Resonance structure for preheating with massless fields, Phys. Rev. D **57**, 702 (1998).

[107] P. Greene, L. Kofman, A. Linde, and A. Starobinsky, Structure of resonance in preheating after inflation, Phys. Rev. D **56**, 6175 (1997).

[108] *Handbook of Mathematical Functions*, edited by M. Abramowitz and I. Stegan (Dover, New York, 1965).

[109] S. Weinberg, *Cosmology* (Oxford University Press, New York, 2008).

[110] S. Carroll, *Spacetime and Geometry* (Addison-Wesley, New York, 2004).

[111] L. Kofman, A. Linde, and A. Starobinsky, Towards the theory of reheating after inflation, Phys. Rev. D **56**, 3258 (1997).

[112] B. A. Bassett, F. Tamburini, D. I. Kaiser, and R. Maartens, Metric preheating and limitations of linearized gravity, Nucl. Phys. **B561**, 188 (1999).

[113] M. P. Hertzberg, J. Karouby, W. G. Spitzer, J. C. Becerra, and L. Li, Theory of self-resonance after inflation. Part 1: Adiabatic and isocurvature Goldstone modes, Phys. Rev. D **90**, 123528 (2014); Theory of self-resonance after inflation. Part 2: Quantum mechanics and particle-antiparticle asymmetry, Phys. Rev. D **90**, 123529 (2014).

[114] X. Gao, T. Li, and P. Shukla, Cosmological observables in multifield inflation with a non-flat field space, J. Cosmol. Astropart. Phys. 10 (2014) 008.

[115] S. Renaux-Petel and K. Turzynski, Geometrical Destabilization of Inflation, Phys. Rev. Lett. **117**, 141301 (2016).

[116] B. R. Greene, T. Prokopec, and T. G. Roos, Inflation decay and heavy particle production with negative coupling, Phys. Rev. D **56**, 6484 (1997).

[117] B. A. Bassett, C. Gordon, R. Maartens, and D. I. Kaiser, Restoring the sting to metric preheating, Phys. Rev. D **61**, 061302 (2000).

[118] M. Gleiser, Pseudo-stable bubbles, Phys. Rev. D **49**, 2978 (1994); E. J. Copeland, M. Gleiser, and H.-R. Mueller, Oscillons: Resonant configurations during bubble collapse, Phys. Rev. D **52**, 1920 (1995).

[119] M. A. Amin, R. Easther, and H. Finkel, Inflaton fragmentation and oscillon formation in three dimensions, J. Cosmol. Astropart. Phys. 12 (2010) 001; M. A. Amin, R. Easther, H. Finkel, R. Flauger, and H. P. Hertzberg, Oscillons after Inflation, Phys. Rev. Lett. **108**, 241302 (2012).

[120] S.-Y. Zhou, E. J. Copeland, R. Easther, H. Finkel, Z.-G. Mou, and P. M. Saffin, Gravitational waves from oscillon preheating, J. High Energy Phys. 10 (2013) 026; S.-Y. Zhou, Gravitational waves from Affleck-Dine condensate fragmentation, J. Cosmol. Astropart. Phys. 06 (2015) 033.

[121] K. D. Lozanov and M. A. Amin, Equation of State and Duration to Radiation Domination after Inflation, Phys. Rev. Lett. **119**, 061301 (2017).

[122] D. G. Figueroa and F. Torrenti, Parametric resonance in the early universe: A fitting analysis, J. Cosmol. Astropart. Phys. 02 (2017) 001.